REAL-TIME OBSERVATION OF MOLECULAR REACTION MECHANISM OF HALOPYRIMIDINES AS RADIO-/PHOTOSENSITIZING DRUGS BY USING TIME-RESOLVED FEMTOSECOND LASER SPECTROSCOPY

by

Chunrong Wang

A thesis
presented to the University of Waterloo
in fulfillment of the
thesis requirement for the degree of
Master of Science.
in
Physics

Waterloo, Ontario, Canada, 2007

I hereby declare that I am the sole author of this thesis. This is a true copy of the thesis, including any required final revisions, as accepted by my examiners.

I understand that my thesis may be made electronically available to the public.

Abstract

Replacement of thymidine in DNA by halopyrimidines, such as bromodeoxyuridine (BrdU) and iododeoxyuridine (IdU), has long been known to enhance DNA damage and cell death induced by ionizing/UV radiation, but the mechanism of action of halopyrimidines at the molecular level is poorly understood. We have applied advanced time-resolved femtosecond laser spectroscopy to this molecular system of biological, chemical and medical significance. We obtained the first real-time observations of the transition states of the ultrafast electron transfer (UET) reactions of halopyrimidines with the ultrashort-lived precursor to the hydrated electron, which is a general product in ionizing/UV radiation. Our results provide a mechanistic understanding of these photo-/radiosensitizing drugs at the molecular level.

We found that the UET reaction of BrdU is completed within 0.2 picosecond (ps) after the electronic exciataion, leading to the formation of the transition state $BrdU^{*-}$ with a lifetime of ~1.5 ps that then dissociates into Br^- and a high reactive radical $dU^{\bullet}$. We have also demonstrated that the reaction efficiency for the formation of the reactive radical $dU^{\bullet}$ to cause DNA damage and cell death is in the order of IdU>>BrdU>CldU>>FdU. This is due to the availability of two precursor states of ~0.2 ps and ~ 0.54 ps lifetimes for dissociative electron attachment (DEA) to IdU, of one precursor state of ~0.2 ps lifetime for DEAs to BrdU and CldU, and no precursors for DEA to FdU. This explains why BrdU and IdU were found to be effective radio-/photosensitizers and indicates that IdU should be explored as the most effective radiosensitizer among halopyrimidines. Moreover, as a by-product of this project, these halopyrimidines have been employed as quantum-state-specific molecular probes to resolve a long-standing controversy about the nature and lifetimes of prehydrated electrons. These findings also have a broader significance as they indicated that nonequilibrium precursor electrons may play an important role in electron-initiated reactions in many biological, chemical and environmental systems.

We have also demonstrated UET reactions of nucleotides with the precursor to the hydrated electrons. Our results indicate that among DNA bases, adenine is the most efficient electron trapper and an effective electron transfer promoter, while guanine is the most effective in dissociative electron attachment. These results not only primarily explain the sequence selectivity of duplex DNA containing BrdU/IdU, but imply that the DEA of guanine is an important mechanism for radiation-induced DNA damage in ionizing radiation and radiotherapy of cancer.

Acknowledgments

I am extremely grateful to Prof. Qing-Bin Lu, for his invaluable supervision and encouragement during my work. His profound guidance and great patience were indispensable to my successful completion of my M.Sc. study and research. In particular, his foresighted sense to numerous scientific issues and devoted attitude to scientific research have inspirited me to go on my probe into science.

My gratitude also goes to all the members of our group for their kind help and friendship.

Thanks are also due to my good friends, Hai-Tang Wang, Xi Chen, Ting Lu, Mei-Jun Lu, Ting Luo, and Li Zhuang, for their encouragement and help.

I am also indebted to Judy McDonnell for providing valuable help. I would also like to thank all the staff members and postgraduate students of the department for their hospitality, help and friendship.

Finally, financial supports to this project from the Canadian Institutes of Health Research (CIHR) are acknowledged.

To my parents

Contents

List of Figures

List of Tables

.

Chapter 1

Introduction

More than one century ago, the Swedish Chemist Svante Arrhenius first concluded that there must exist an intermediate in the transformation from reactants to products. Later, this intermediate came to be known as the transition state. We need to know the properties of the transition state if we are to predict, understand and modify the course of a reaction. Real-time observations of molecular reactions are of great importance in diverse fields from chemistry and biology to medicine. *Time-resolved ultrafast laser spectroscopy* is the most versatile and powerful technology for real-time observation of molecular reactions. It uses laser flashes of such ultrashort duration down to the time scale on which the reactions actually happen - femtoseconds (fs) (1fs= 10^{-15} seconds) [1]. The application of this spectroscopy to chemistry has led to the birth of a field in chemistry, the so-called *femtochemistry* [1]. Most recently, this spectroscopy has been extended to investigate structural and reaction dynamics of biological systems, including DNA, RNA and proteins [2-6]. New exciting multidisciplinary frontiers, *ultrafast biophotonics, femtobiology and femtomedicine,* which involve a fusion of ultrafast laser spectroscopy with biology/medicine, are being developed.

Halopyrimidines, particularly 5-Bromo-2'-deoxyuridine (BrdU) and 5-Iodo-2'-deoxyuridine (IdU), are the most important hypoxic radiosensitizing drugs in radiotherapy of cancer. As potential radiosensitizers, they have passed phase I-II clinical trials, but they failed in phase III clinical trials. This is probably due to the poorly understanding of the molecular reaction mechanism of these drugs. This thesis work presents a new mechanistic understanding at the molecular level of halopyrimidines as radiosensitizing drugs, using the advanced time-resolved femtosecond laser spectroscopy. The transition states of the ultrafast electron transfer reactions of halopyrimidines with nonequilibrium prehydrated electrons are directly observed and a novel molecular reaction mechanism is presented in this thesis.

1.1 Current status of cancer research

Cancer diseases represent a serious public health problem since they affect many people, involve severe symptoms, and are a frequent cause of death. Many people experience these diseases as being more frightening than other conditions that may have a worse prognosis. Cancer results from abnormal growth of otherwise healthy cells. Cancer cells continue to grow and divide without restraint, eventually spreading throughout the body, interfering with the function of normal tissues and organs, and progressively leading to

death [7-9]. Cancer as a disease in the human population is becoming a larger health problem due to the increasing in aging and the medicines used as treatments have clear limitations [10].

Typically when a cancer is physically detected, it has been developing for a certain period of time. As time equates with increased cellular changes towards aggressiveness, it follows that the earlier a cancer can be detected, the fewer changes it has resulted in and the more likelihood there will be of getting a good response to treatment. Early detection of very small or pre-malignant growths should result in more cures. It is possible to screen vulnerable populations for the pre-malignant signs or early stages of some cancers. Screening large numbers of people for early signs of cancer should therefore be beneficial, provided that a suitable test is available. In order to be effective, such screening must be applied to all the population at risk; it is useful only in cancers where there is a reasonable chance of a cure. Screening is expensive, and so it is used only for a few cancers and only in countries that can afford it. When pre-malignant or early malignant stages are detected by screening, prompt treatment can halt the progress of the disease. It is more usual that the patient detects symptoms and reports these to a doctor, who then makes a preliminary diagnosis and refers the patient to a hospital with specialised staff and better diagnostic tools. Hospital examination may include imaging, biopsy to provide material for histopathology and clinical biochemistry. If the diagnosis is confirmed, then the state of development of the cancer (staging) is established, because the type of treatment is determined by the stage [7-9].

As cancer therapy is radical and involves several types of treatment, it is delivered by teams of specialists working in large hospitals. The principal therapeutic modalities are surgery, **radiotherapy**, **chemotherapy** and the emerging **photodynamic therapy** (PDT), although other disciplines such as imaging, nursing and psychology provide important components in the whole treatment.

Surgery, commonly combining with radiotherapy, is the primary treatment method for most cancers, and also for later removal of tumour residuals or recurring tumours. The primary aim of surgery is to remove the entire tumour and, when appropriate, any metastases in regional lymphatics. This is the cornerstone of treatment for solid tumours, and it can, in some cases, result in a complete cure. In earlier times, cancer surgery often resulted in undesirable loss of function and deformities; more recently, there has been a trend to minimise surgery and to retain as much form and function as possible. A good example of this conservative trend is provided by the current therapy for breast cancer. In the past, radical mastectomy provided an adequate means of local control; however, the consequent effects could involve other organs and were often psychologically traumatic. Currently, partial mastectomy (lumpectomy) with adjuvant therapy is favoured because it provides a means of control that is as good as that provided by radical mastectomy,

without the mutilating effects. The use of imaging techniques to define the size and position of deep-seated tumours and their surrounding organs can provide important information before surgery and radiotherapy. Such advances have led to an improvement in outcome of cancers such as that of the stomach, where surgery is essentially the only possible curative treatment [7-9].

The objective of radiotherapy is to deliver a defined radiation dose to a specific tissue volume — including the tumour and adjacent tissues where tumour cells might be found –with the intent to kill tumour cells while minimizing irradiation of surrounding, healthy tissue. Radiotherapy generates DNA strand breaks through free-radical formation. Due to its more relevance to the work of this thesis, radiotherapy will be discussed in more detail in the next section.

The term “chemotherapy” is conventionally confined to the use of cytotoxic or cytostatic drugs that respectively kill malignant cells or prevent them from proliferating. The efficacy of such drugs depends on the concentration of the drug reaching the tumour, the duration of exposure, and the proportion of the population that is proliferating. The latter point is important, as the drugs act mainly on proliferating cells and tumours commonly include subpopulations of cells that are not dividing. This action is not limited to malignant cells; it affects proliferating cells throughout the body, resulting in numerous down-stream effects. Chemotherapy almost inevitably causes depression of the haemopoietic system. This means a reduced output of blood cells, which result in reduced resistance to disease, anaemia and thrombocytopenia (reduced number of platelets). Generally, chemotherapeutic drugs cause severe toxic side effects, e.g., they can specifically toxic to vital organs such as the heart and the kidney. So they must be used with utmost caution. To some degree, the side effects can be minimised by careful dosing, by using combinations of drugs with different toxicities or therapies (combination therapy) and by using supportive procedures. During the course of treatment, the target cells may become resistant to the drugs used, and so many chemotherapists prefer to use high doses initially in the hope of killing all the malignant cells before resistance develops [7-9].

Solid tumours are the most formidable cancer to be cured. In the case of solid tumours, the first step is usually surgical removal of the primary cancer together with a margin of normal tissues, as such cancers are commonly irregular in shape. Then radiotherapy is applied to the area around the site to destroy any possible remnants of the tumour. At the same time, cytotoxic drugs can be given to kill residual cancer cells and possible metastases. In such circumstances, the secondary treatments are referred to as adjuvant therapy; they are not the major modality, but they are an essential supplement to back it up. This is the usual pattern of treatment, but there are some situations where alternative approaches are used. In regions of anatomical complexicity, such as the head and neck,

and in regions of vital biological function, such as the brain and spine, surgery would cause many problems, and so radiotherapy is sometimes the preferred modality. In disseminated cancers such as leukaemia, the only modality that can be used is chemotherapy [7-9].

Photodynamic therapy (PDT) is emerging as a novel clinical approach that uses lasers and drugs (photosensitizers) for the treatment of various tumors and other non-malignant conditions, such as age related macular degeneration, and has great potential for applications in regenerative medicine [11]. PDT has potential advantages over surgery and other therapies: it is comparatively non-invasive, can be targeted accurately and has fewer side effects. Visible light on its own does not damage cells, but it can have deleterious effects in the presence of light-sensitive (photosensitive) chemicals such as porphyrins plus oxygen. Naturally occurring porphyrins such as haemoglobin bind and transport oxygen (O_2). In the laboratory, haemoglobin can be modified with acid so that it can absorb light in the 630nm (red) region of the spectrum to provide energy transfer from the photosensitive porphyrin to oxygen and generate the reactive superoxide radical $O_2\cdot$. The porphyrin is thus a prodrug. Only cells containing porphyrin are directly destroyed. Photodynamic therapy has been adapted such that the porphyrin is given systemically and the target cancer is illuminated with 630nm light focused on the cancer and not the surrounding tissues. The most commonly used photosensitizer is porfimer sodium, a partially purified haematoporphyrin derivative. Photodynamic therapy has been used successfully to treat cancers of the bladder, head and neck, and oesophagus. Currently, most photosensitizers in clinical applications are photoactivated using a light source in the range 630-690 nm. At this wavelength, the largest attainable depth of PDT-induced cellular changes could reach up to 15 mm, but in most cases it is much less than half of that. For this reason, the increase of light penetration is considered to be an important factor in increasing the clinical efficacy of PDT. This is one of the focuses of current research [11].

Biological treatment refers to a general concept involving the attempts to treat cancer by engaging the body's own natural systems. Important approaches include strengthening the immune defense, stimulating new blood formation, and anticipated opportunities in **genetic therapy**. Although progress in this area has been substantial, these forms of therapy can not yet be considered as significant as surgery, radiotherapy and chemotherapy [7-9].

In spite of intense studies over decades, the main curative therapy for cancer – surgery and radiotherapy — is generally only successful if the cancer is found at an early localized stage. Existing chemotherapeutic treatments are largely palliative in advanced tumours. Often chemotherapy is effective only for a certain period of time. Toxic side effects are also a common issue. These drawbacks have even prompted the call to

identify molecular mechanisms of human cancers and to design therapeutics that target these mechanisms instead [10]. In the development of new drugs, several issues need to be addressed, including improved and durable antitumour efficacy, reduced toxic side effects and prevention of drug resistance [10]. However, most of the molecular mechanisms of action, toxicity and resistance in existing effective drugs are still poorly understood [12, 13]. The tradition approach for anticancer drug discovery is to synthesize a large number of drug analogue compounds and then to do bioactivity and cytotoxicity screening. It is estimated that more than 10,000 compounds need to be screened in order to obtain one new, effective anticancer drug [14]. *Overall, the identification of successful anticancer agents with clinical utility has remained a somewhat empirical process* [10]. There is a strong need for a mechanistic understanding of action of existing drugs *at the molecular level*, which can, in turn, lead to mechanism-based design of new drugs [10].

1.2 Radiotherapy

Most therapeutic radiography uses specialised apparatus that delivers a narrow beam of high-energy X-rays to a well-defined area of the body. This allows treatment of both superficial and deep-seated tumours without surgical trauma. Damage to the adjacent and overlying tissues is minimised by selective shielding and by varying the direction of the beam so that the total dose occurs only at the site of the tumour and adjacent organs, together with the use of stereotactic apparatus and computer-aid planning of irradiation. This is important because some organs such as the lens of the eye, the spinal cord, the lung, the kidney and the small intestine, have a poor capacity to repair radiation damage [7-9].

The desired outcome of radiotherapy is to kill malignant cells by causing irreparable damage to their DNA. Cycling cells are radiosensitive, but tumour stem cells or quiescent G_0 cells are relatively resistant. Because of this issue, radiation doses are fractionated, so that the total dose is delivered over a period of days. This allows any damaged normal tissues to repair themselves while the tumour stem cells become reoxygenated and start proliferating. Subsequent doses will then destroy the reactivated tumour cells. Reoxygenation is also important, as oxygen is required for the generation of the free radicals necessary to produce full effectiveness (oxygen effect will be discussed in more detail below) [7-9].

Less commonly, radiotherapy involves the use of radio-cobalt sources can be used to provide a beam of gamma rays for external radiotherapy. Another application is brachytherapy, which uses radiation from radioactive sources either placed closed to or inserted in the tumour. Plastic-covered flexible iridium-131 wires can be inserted into

tumours of the tongue, breast, brain and buccal mucosa to produce effects similar to those produced by external radiotherapy systems [7-9].

In radiotherapy, ionizing radiation is used to kill tumour cells. The principal means by which ionizing radiations dissipate their energy in matter is by the ejection of orbital electrons from atoms. The removal of one or more of these orbital electrons is called ionization. Because each electron is hold within its orbit by a specific binding energy, work must be done to when any orbital electron is removed. Atoms are electrically neutral, but when they are ionized the loss of an orbital electron leaves them positively charged. The ionized atom and the dislodged electron constitute an ion pair [15, 16].

Not every interaction between ionizing radiation and matter need result in ionization. Excitation, a less drastic process than ionization, may also occur. In it an electron in an atom is raised to a higher energy state, moved to a more distant orbit, but not ejected. Excitation is the most important mode of energy dissipation by ultraviolet light, and probably forms a significant percentage of the energy dissipated by ionizing radiation in tissue [15, 16].

Ionization produced by radiation is a random process; ordinarily, an ionizing particle will have sufficient energy to remove an orbital electron from any atom with which it chances to interact. Any atom, without preference, may lose an electron in this way and is itself, ionized. The randomness-the nonselectivity of the process is in sharp contrast to the action of radiations of low-energy (Ultraviolet) which are absorbed selectively by certain molecules and have no effect on others. The transfer of energy from lower-energy radiations, unlike that of ionizing radiation, is not random and will occur only with certain atoms or molecules, even at times, with a small portion of a molecule [15, 16].

If a complex system (one consisting of more than one kind molecule) is irradiated with any of the ionizing radiations, then, because the nature of the energy exchange is random, ionization is most likely to occur in those kinds of molecules that are present in the largest number. When cells or tissues are irradiated, most of the radiation energy is absorbed by water, because cells are made up of more than 70% water. As will be shown below, there are essentially three different species formed in the radiolysis of water, the OH radical, the solvated electron (e_{aq}^-) and the H-atom.

The two major processes of the interaction of ionizing radiation with matter are ionization and electronic excitation. In liquid water these reactions are described by reactions 1 and 2 [15, 16]:

$$H_2O \rightarrow H_2O^+ + e^- \quad (1)$$

$$H_2O \rightarrow H_2O^* \quad (2)$$

The water radical cation is a strong acid and rapidly loses a proton to the surrounding water molecules (reaction 3). The electron becomes solvated within a very short time (reaction 4):

$$H_2O^+ + H_2O \rightarrow H_3O^+ + OH^\cdot \quad (3)$$

$$e^- + n\,H_2O \rightarrow e_{aq}^- \quad (4)$$

The excited water molecules formed in the second primary process (reaction 2) can break up into H-atoms and OH radicals or form an electron (reaction 5):

$$H_2O^* \rightarrow H^\cdot + OH^\cdot \text{ or } H_2O^+ + e^- \quad (5)$$

The free radicals($OH^\cdot$, and $H^\cdot$) either react with one another within the spur or diffuse into the bulk of the solution, reacting with anything that they encounter, producing H_2O, H_2O_2, molecular hydrogen and some other free radicals such as $HO_2\cdot$(hydrogen peroxide). The major products of water radiolysis are OH•, e_{aq}^-, H•, H_2O_2 and H_2, whose yields per 100 eV energy deposited are 2.4, 2.8, 0.4, 0.8 and 0.4, respectively. Most importantly, in the living system, these free radicals may react with organic molecules-the molecules of which cells and tissues are built — and change them. The following equations illustrate how this may come about.

$$HO_2^\cdot + RH \rightarrow R^\cdot + H_2O_2 \quad (6)$$

$$RH + HO_2^\cdot \rightarrow RO^\cdot \text{ (an organic free radical)} + H_2O \quad (7)$$

If RH in either of these cases is a fundamental organic molecule — one important in the metabolism of the cell, either as a building block or as a finished product — an upset in the chemistry or the metabolism of the cell can be expected. In addition, H_2O_2 is a cell poison and if present in sufficient quantities can materially interfere with metabolism. Organic free radicals may represent not only changed molecular constituents of the cell, but also substances that are free to attack other constituents and generate further molecular changes.

The presence of oxygen during irradiation enhances the magnitude of radiation effects. These effects are of sufficient importance to merit special treatment. In the biological system, oxygen reacts with the free radicals produced by radiation and draws them into further destructive, auto-oxidative chain reactions with the molecules of cells. It is also very possible that oxygen can block restoration of an intact molecule by interacting with radiation-produced organic free radicals which might otherwise have been restored to its normal state. Thus the effect of radiation can also be enhanced by prevention of some fraction of the expected restoration. Finally, the presence of oxygen at irradiation will

greatly promote the formation of hydrogen peroxide and organic peroxide [15, 16].

The processes described above are the initiating events leading to damage — the transfer of energy from ionizing radiation to the substance of the cell (ionization) and the subsequent transfer of this energy among the molecules of the substance (free radicals, oxygen effect). Follow these initiating events, alternation in structure and function at much higher levels of organization is detected at some later time after irradiation of a living system.

The basic concept under which there is an application of the oxygen effect in radiotherapy rests on the premise that certain tumours have hypoxic (radioresistant) regions when compared to normal tissue and even to other regions of the same tumour. Even though tumours, with their large numbers of dividing cells, are, in many cases, more sensitive to radiation than the more static normal tissues that surround them, regions of poor oxygenation within tumours, particularly solid tumours, might make some of the cells quite insensitive to radiation — insensitive enough to survive the usual forms of radiotherapy.

It has been accepted for a long time that DNA damage and tumour cell death in ionizing radiotherapy are caused mainly by OH and H_2O_2, while electrons would play only a minor role. However, a recent important study has shown that low-energy free electrons in energies of 1-20 eV can cause significant DNA damage via formation of transient anion resonances [17]. More remarkably, the free radicals produced in ionizing radiation need oxygen to produce a full radiotherapy effect, as mentioned above. In contrast, the electrons produced in the ionizing radiation have the radiotherapy effect without the need of oxygen and thus can play an important role in the hypoxic regions of the living system.

Moreover, in order to minimize side effects and enhance radiotherapeutic efficacy, radiosensitizing drugs are often used in combination with ionizing radiation. The mechanism for the radiosensitivity enhancement is generally related to the reactions of electrons with the sensitizing drugs. The application of radiosensitizers is especially beneficial to hypoxic tumours.

1.3 Halopyrimidines as radiosensitizing drugs

Halopyrimidines, e.g., bromodeoxyuridine (BrdU) and iododeoxyuridine (IdU), are most important hypoxic sensitizers in radiotherapy of cancer. Replacement of thymidine in DNA by BrdU/IdU has long been known to enhance DNA damage induced by ionizing radation (γ- or x-ray) [18-27]. In 1958, Zamenhof, DeGiovanni and Greer observed that

bacterial cells containing DNA in which thymine is replaced by bromouracil (BrU) become more sensitive to ionizing radiation than their unsubstituted counterpart [18]. This report led to an important application: the treatment of tumors by combining incorporation of halopyrimidines into DNA and ionizing radiation. Since then, much work has been devoted to understanding the mechanism by which these radiosensizers operate [19-27].

Incorporation into DNA is a prerequisite for radiosensitization of human tumors by the halogenated thymidine analogues, and the extent of radiosensitization correlates directly with the percentage of thymidine substitution in DNA [25, 26]. Halogenated pyrimidine analogues are incorporated into actively dividing cells and substitute for thymidine in DNA. As a result of thymidine substitution in DNA, tumor cells are more sensitive to the lethal effects of radiation. The sensitivity to irradiation of cells that have incorporated (BrdU) increases about two to three times [27].

Also, replacement of thymine in DNA by BrdU/IdU has long been known to enhance photosensitivity with respect to single- and double-strand breaks, creation of alkali-labile sites and DNA-protein photo-cross-linking, by forming uracilyl radical [28-29]. The enhancement of DNA damage caused by UV-irradiation of duplex containing BrdU/IdU has received considerable attentions, and it was observed that the BrdU/IdU enhanced DNA damage shows significant nucleic acid sequence dependence [29, 30].

In addition, halopyrimidines have also been exploited to probe protein-nucleic acid interactions and nucleic acid structure via inducing DNA/RNA-protein *photocrosslinking* [34-37]. The results reported by Tad H. Koch and coworkers demonstrated that site-specific substitution of certain nucleotides with BrdU/IdU greatly increased the photo-cross-linking yield and substitution favoring a specific protein-DNA cross-links [36, 37]. The ability of BrdU/IdU and other 5-halopyrimidine nucleosides to form protein-nucleic acid cross-links has been exploited for mapping protein-nucleic acid interactions [34-37]. The 5-halopyrimidine nucleosides' sensitivity to UV-irradiation has been exploited in the application of these molecules as structural probes of protein-nucleic acid interactions and nucleic acid structure [34-37].

Identified as a potential sensitizer for radiotherapy of cancer, halopyrimidines have been tested in several Phase I - III clinical trials [38-40]. Some clinical studies have demonstrated the ability of BrdU to radiosensitize malignant brain tumors [38]. The result of recent phase I-II clinical trials using infusion of BrdU or IdU before and during radiation therapy suggest an improved outcome compared to radiation alone [39]. However, Phase III clinical trials failed [40]. Generally the clinical results have not been satisfactory and therefore no XdUs have been approved for clinical use. This is probably due to poor understanding of the mechanism of the radiosensitivity

enhancement. Although lots of investigations dedicated to the understanding of the mechanism(s) by which these halopyrimidines operate, the molecular reaction mechanism of these drugs in their early physio-chemical steps is still poorly understood.

1.4 The major objectives of this thesis

The major objective of the proposed work in this thesis is to obtain a mechanistic understanding at the molecular level of halopyrimidnes as the most important hypoxic radiosensitzing drugs, using the advanced time-resolved femtosecond laser spectroscopy. Real-time observations of how the molecular reactions of halopyrimidines lead to the formation of reactive radicals should provide important information for a mechanistic understanding of these anticancer drugs leading to the radio-/photo-sensitization enhancement. This understanding has the great potential to improve therapeutic effects of these drugs. Moreover, with the knowledge, it will be possible to design new drugs that can effectively treat many types of tumours with reduced toxic side effects and no or little resistance.

1.5 Structure of this thesis

Following this introduction, the principle of time-resolved femtosecond (fs) laser spectroscopy is described in chapter 2. Chapter 3 gives a description of direct observation of the transition state of ultrafast electron transfer reactions of BrdU with the prehydrated electron. In chapter 4, the experimental results for the studies extending to four halopyrimidines including FdU, CldU, BrdU and IdU are presented and the reaction mechanism for the radio-/photosensitization is addressed, together with a discussion on the physical nature of the prehydrated electron. Then the reaction transition states of prehydrated electrons with nucleotides is shown and discussed in chapter 5. Finally, the conclusions drawn from this work are summarized in chapter 6.

References:

1. A. H. Zewail, “Femtochemistry: Atomic-Scale Dynamics of the Chemical Bond Using Ultrafast lasers (*Nobel Lecture*)”, Angew. Chem. Int. Ed. **39**, 2586(2000).
2. C. Z. Wan, T. Fiebig, S. O. Kelley, C. R. Treadway, J. K. Barton, and A. H. Zewail**,** “Femtosecond dynamics of DNA-mediated electron transfer”, Proc. Natl. Acad. Sci. USA **96**, 6014(1999).
3. S. O. Kelley, and J. K. Barton, “Electron transfer between bases in double helical DNA”, Science **283**, 375(1999).

4. J. K. A. Kamal, L. Zhao, and A. H. Zewail, “Ultrafast hydration dynamics in protein unfolding: Human serum albumin”, Proc. Natl. Acad. Sci. USA **101**, 13411(2004).
5. T. Brixner, J. Stenger, H. M. Vaswani, M. Cho, R. E. Blankenship, and G. R. Fleming, “Two-dimensional spectroscopy of electronic couplings in photosynthesis”, Nature **434**, 625(2005).
6. C. E. Crespo-Hernandez, B. Cohen, and B. Kohler, “Base stacking controls excited-state dynamics in A-T DNA”, Nature **436**, 1141(2005).
7. G. M. Cooper, “The Cancer Book”, (Boston, London, 1993).
8. M. Blasco, C. J. Norbert, et.al, “The Molecular Biology Of Cancer”, edited by Stella Pelengaris and Michael Khan (2006).
9. R. J. B. King, and M. W. Robins, “Cancer Biology”, Third edition (2006).
10. J. B. Gibbs, “Mechanism-Based Target Identification and Drug Discovery in Cancer Research”, Science **287**, 1969(2000).
11. P. N. Prasad, “Introduction to Biophotonics”, (New Jersey, 2003).
12. J. Reedijk, “New clues for platinum antitumor chemistry: Kinetically controlled metal binding to DNA”, Proc. Natl. Acad. Sci. USA **100**, 3611(2003).
13. M. F. Fuertes, C. Alonso, and J. M. Perez, “Biochemical Modulation of Cisplatin Mechnisms of Action: Enhancement of Antitumor Activity and Circumvention of Drug Resistance”, Chem. Rev. **103**, 645(2003).
14. E. R. Jamieson and S. J. Lippard, “Structure, Recognition, and Processing of Cisplatin-DNA Adducts”, Chem. Rev. **99**, 2467(1999), and references therein.
15. D. J. Pizzarello, and R. L. Witcofski, “Basic Radiation Biology” (1967).
16. C von Sonntag, “The Chemical Basis of Radiation Biology”, (London - New York – Philadelphia, 1987).
17. B. Boudaiffa, P. Cloutier, D. Hunting, M. A. Huels and L. Sanche, “Resonant Formation of DNA strand breaks by low-energy (3-20 eV) electrons”, Science **287**, 1658(2000).
18. S. Zamenhof, R. DeGiovanni, and S. Greer, “Incorporation of halogenated pyrimidine into the deoxyribonucleic acid of bacterium E. coli and its bacteriophages”. Nature **181**, 827(1958).
19. W. C. Dewey, B. A. Sedita, and R. M. Humphrey, “Radiosensitization of X chromosome of Chinese hamster cells related to incorporation of 5-bromodeoxyuridine” Science **152**, 519(1966).
20. W. C. Dewey and R. M. Humphrey, “Increase in radiosensitivity to ionizing radiation related to replacement of thymidine in mammalian cells with 5-bromodeoxyuridine”. Radiat. Res. **26**, 538(1965).
21. K. Sano, T. Hoshino and M. Nagai, “Radiosensitization of brain tumor cells with a thymidine analogue (Bromouridine)”. J. Neurosurg. **28**, 530(1968).
22. C. F. Webb, G. D. D. Jones, J. F. Ward, D. J. Moyer, J. A. Aguilera, and L. L. Ling “Mechanisms of Radiosensitization in Bromodeoxyuridine-substituted Cells”, Int. J. Radiat. Biol. **64**, 695(1993).

23. L. L. Ling, and J. F. Ward, “Radiosensitization of Chinese hamster V79 cells by bromodeoxyuridine substitution of thymidine: enhancement of radiation-induced toxicity and DNA strand break production by monofilar and bifilar substitution”, Radiat. Res. **121**, 76(1990).
24. C. L. Limoli, and J. F. Ward, “A new method for introducing double-strand breaks into cellular DNA”, Radiat. Res. **134**, 160(1993).
25. B. Djordjevic and W. Szybalski, “Genetics of human cell lines: III. Incorporation of 5-bromo- and 5-Iododeoxyhridine into the deoxyribonucleic acid of human cells and its effect on radiation sensitivity”, J. Exp. Med. **112**,509 (1960) and references therein.
26. T. J. Kinsella, P. P. Dobson, J. B. Mitchell, and A. J. Jr. Fornace, “Enhancement of X-ray induced DNA damage by pre-treatment with halogenated pyrimidine analogs”, Int. J. Radiat Oncol. Biol. Phys. **13**, 733 (1987).
27. M. D. Prados, C. Scott, et. al, “A Phase 3 randomized study of radiotherapy plus procarbazine, CCNU, and Vincristine (PCV) with or without BUdR for the Treatment of Anaplastic Astrocytoma: A Preliminary Report of RTOG 9404”, Int. J. Radiation Oncology Biol. Phys. **45,** 1109(1999), and references therein.
28. H. Sugiyama, K. Fujimoto, and I. Saito, “Evidence for intrastrand C2’ hydrogen abstraction in photoirradiation of 5-Halouracil-Containing Oligonucleorides by using stereospecifically C2’-deuterated deoxyadenosine”, Tetrahedron Letters **37**, 1805(1996).
29. H. Sugiyama, Y. Tsutsumi, and I. Saito, “Highly sequence-selective photoreaction of 5-bromouracil-containing deoxyhexanucleotides”, J. Am. Chem. Soc. **112**, 6720(1990)
30. T. Chen, G. P. Cook, A. T. Koppisch, and M. Greenberg, “Investigation of the origin of the sequence selectivity for the 5-Halo-2’-deoxyuridine sensitization of DNA to damage by UV-irradiation”, J. Am. Chem. Soc. 122, 3861(2000)
31. H. Sugiyama, Y. Tsutsumi, K. Fujimoto, and I. Saito, **“**Photoinduced deoxyribose C2' oxidation in DNA. Alkali-dependent cleavage of erythrose-containing sites via a retroaldol reaction”. J. Am. Chem. Soc. **115**, 4443(1993).
32. H. Sugiyama, K. Fujimoto, and I. Saito, “Stereospecific 1,2-Hydride Shift in Ribonolactone Formation in the Photoreaction of 2'-Iododeoxyuridine”, J. Am. Chem. Soc. **117**, 2945(1995).
33. G. P. Cook and M. M. Greenberg, “A novel mechanism for the formation of direct strand breaks upon Anaerobic photolysis of duplex DNA containing 5-Bromodeoxyuridine”, J. Am. Chem. Soc. **118**, 10025 (1996) and references therein.
34. KL Wick and KS Matthews, “Interactions between lac repressor protein and site-specific bromodeoxyuridine-substituted operator DNA. Ultraviolet footprinting and protein-DNA cross-link formation”, J. Biol. Chem. **266**, 6106(1991).

35. E. E. Blatter, Y. W. Ebright, and R. H. Ebright, “Identification of an amino acid–base contact in the GCN4–DNA complex by bromouracil-mediated photocrosslinking”, Nature **359**, 650(1992).
36. M. C. Willis, B. J. Hicke, O. C. Uhlenbeck, T. R. Cech and T. H. Koch, “Photocrosslinking of 5-iodouracil-substituted RNA and DNA to proteins”, Science **262**, 1255(1993).
37. B. J. Hicke, M. C. Willis, T. H. Koch, and T. R. Cech, “Telomeric Protein-DNA Point Contracts Identified by Photo-Crosslinking Using 5-Bromodeoxyuridine”, Biochemistry **33**, 3364(1994)
38. M. Matsutani, T. Kohno, T. Nagashima, I. Nagayama, T. Matsuda, T. Hoshino, and K. Sano, “Clinical trial of intravenous infusion of bromodeoxyuridine (BUdR) for radiosensitization of malignant brain tumors”, Radiat. Med. **6**, 33(1988).
39. R. Urtasun, T. Kinsella, N. Farnan, J. Del Rowe, S. Lester, and D. Fulton, “Survival improvement in anaplastic astrocytoma, combining external radiation with halogenated pyrimidines: final report of RTOG 86-12, Phase I-II Study”, Int. J. Radiat. Oncol. Biol. Phys. **36**, 1163(1996).
40. M. D. Prados, C. Scott, H. Sandler, J. C. Buckner, T. Phillips, and C. Schultz, “A phase 3 randomized study of radiotherapy plus procarbazine, CCNU, and vincristine (PCV) with or without BUdR for the treatment of anaplastic astrocytoma: a preliminary report of RTOG 9404”, Int. J. Radiation Oncology Biol. Phys. **45**, 1109 (1999), and references therein.

Chapter 2

Experimental method

The major methodology to be applied for this project is time-resolved femtosecond (fs) laser transient absorption spectroscopy. This is the most versatile and powerful technique for real-time observation of molecular reactions and can be described as the world's fastest “camera” [1].

A schematic diagram to illustrate the principle of a fs-resolved laser spectroscopy is shown in Figure2.1. It uses laser flashes of such short duration that we are down to the time scale on which the reactions actually happen - femtoseconds (fs) (1fs= 10^{-15} seconds). The “camera” records what happens in a molecular reaction by initiating the reaction with a femtosecond laser pulse (pump pulse) in a certain color (wavelength) (the reactant molecule is excited into a higher energy state). A short time later a second pulse (probe pulse) in a different color takes a “picture” of the reacting molecules or the newly created species. By successively delaying the probe pulse a “film” is obtained of the course of the reaction. The “camera” gives no direct image of the molecules. Instead, the reacting molecules or new species are observed by measuring certain characteristic properties, e.g., an optical transmission (an absorption spectrum is obtained). The one or more transition states probed (detected) at chosen wavelengths (colors) have specific spectra that serve as fingerprints, and they can therefore be identified and characterized.

Dr. Lu has successfully built a high-sensitivity time-resolved fs laser spectroscopy laboratory in the Department of Physics of the University of Waterloo. Our fs laser amplifier system produces a highly stable laser beam of 1 kHz, 1mJ per pulse and <120 fs pulse width. This amplifier system is accompanied by two optical parametric amplifiers (OPAs), which offer a wide wavelength extension from UV (≥266 nm) to NIR (several um) for the pump and the probe pulses.

In our applications, the pump pulse is used to initiate the reaction or to create a reacting species such as an electron via two-photon excitation of water, while the probe is to detect the intermediate species (transition states) during a reaction, which include a precursor electron, a drug excited state and a drug anionic state formed after capturing an electron. The time delay between the pump and the probe pulses is obtained by a precise microstepping motor stage, and time resolution in fs can therefore be achieved with the use of fs laser pulses (not a long detour needed: the light goes through the distance of 1 μm in 3.3 fs!). The electronics recording the spectrum and the motion controller are integrated into a Labview program that directly gives rise to a transient absorption or fluorescence spectrum (as a function of delay time) to show the real-time evolution of a particular transition state. Once intermediate species are identified, the reaction pathway can be determined. With this information, it is then possible to predict, understand and modify the course of a drug reaction [1-3]. This spectroscopic technique provides us with a unique capability of obtaining real-time observation and control of biochemical reactions in solutions.

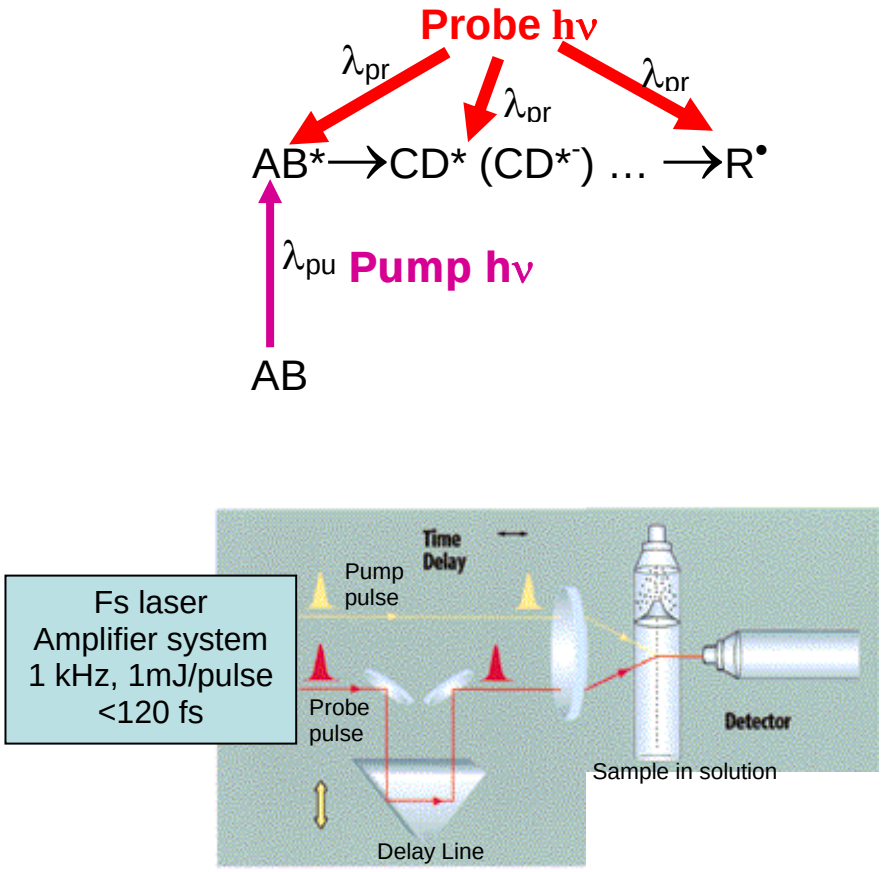

Figure 2.1. Schematic diagram for a fs time-resolved laser spectroscopy

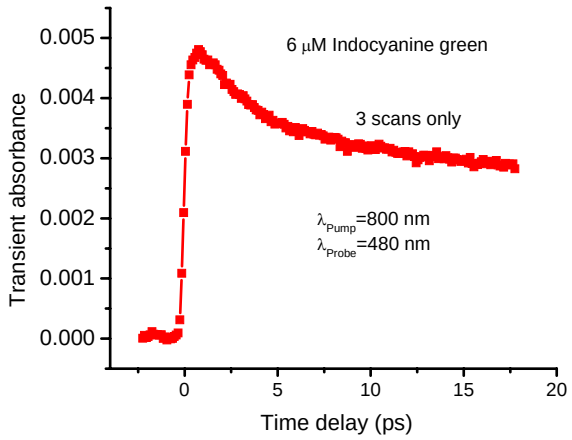

Figure 2.2. High-sensitivity time-resolved femtosecond laser transient absorption spectra of the dynamics of an excited state of a candidate PDT drug (indocyanine green, ICG), where the used pump and probe pulse energies are only 12 and 0.2 nanojoule (nJ), respectively.

Currently, the spectroscopy at our laboratory can detect transient absorbance of as small as 10^{-4} of an intermediate reaction species at the very low pump energy of ≤50 nanojoule (nJ) and the very low probe energy of ≤1 nJ with a time resolution of 20 fs. This is essential to the studies of biomolecules with ultrashort fs laser pulses, where both damage to sample and secondary reactions can be avoided and therefore true initiated reactions of intact drug molecules can be observed in real time.

A typical spectrum is given in Figure 2.2, where the first fs pulse (the pump) at 800 nm was used to excite a candidate PDT drug (ICG) molecule and the second pulse (the probe) at 480 nm coming at varying time delay was used to detect one of the simplest transition states, an excited state (ICG*) of the drug. The dynamics of the transition state can be determined by measuring the decaying lifetime of the species. If there was present another agent, e.g., cisplatin (CDDP), showing reactivity to ICG*, then electron transfer (ET) from ICG* to CDDP is expected and the decay dynamics of ICG* would be changed. By measuring the variation in the lifetime of ICG* as a function of CDDP concentration, we can determine the reaction efficiency (the rate constant). Moreover, a third species can be introduced into the ET reaction, which could promote or quench the ET reaction. Thus, we can monitor the mediating effect of the third agent.

To obtain the precise formation and decay lifetimes of transition-state species, the instrument response function must be taken into account to fit the obtained transient absorption spectra. The time-dependent transient absorption signal is given by a number of exponential functions. These exponential terms are convoluted with the instrument response function repressed by a Gaussian function $G(t) = (1/\sqrt{2\pi}\sigma)\exp(-t^2/2\sigma^2)$, where σ is the standard deviation for the Gaussian and is related to the FWHM (Full Width at Half Maximum) of the pump-probe cross-correlation function by $\sigma = FWHM / 2\sqrt{2\ln 2}$. The resulting time-dependent signal S(t) is given by

$$S(t) = \sum_{i=1}^{n} c_2 \int_{-\infty}^{t} G(t')\exp(-\frac{t-t'}{\tau_i})dt' \qquad (2.1)$$

where negative (positive) c_i is the amplitude of the component i with rising (decay) time τ_i. Eq. (2.1) can be solved analytically to give the following equation [4]:

$$S(t) = \sum_{i=1}^{n} c_i \frac{1}{2}\exp(\frac{\sigma^2}{2\tau_i^2} - \frac{t}{\tau_i}) \times [1 - erf(\frac{1}{\sqrt{2}}(\frac{\sigma}{\tau_i} - \frac{t}{\sigma}))] \qquad (2.2)$$

where erf is the error function. The best fits to the experimental spectra were obtained by using a least-squares fitting program.

Figure 2.3. Experimental setup @ Phys 136, University Of Waterloo

References:

1. Cited from The Royal Swedish Academy of Sciences' illustrated presentation for The 1999 Nobel Prize in Chemistry (http://nobelprize.org/chemistry/laureates/1999/illpres/reaction.html).
2. J. C. Polanyi, "Some Concepts in Reaction Dynamics (*Nobel Lecture*)", Science, **236**, 680(1987).
3. A. H. Zewail, "Femtochemistry: Atomic-Scale Dynamics of the Chemical Bond Using Ultrafast lasers (*Nobel Lecture*)", Angew Chem. Int. Ed., **39**, 2586(2000); J. Phys. Chem. A, **104**, 5660(2000).
4. S. Pedersen, Ph.D. Thesis (California Institute of Technology, 1996).

Chapter 3

Direct observation of the transition state of ultrafast electron transfer reaction of BrdU with the prehydrated electron

Table of Contents Graphic

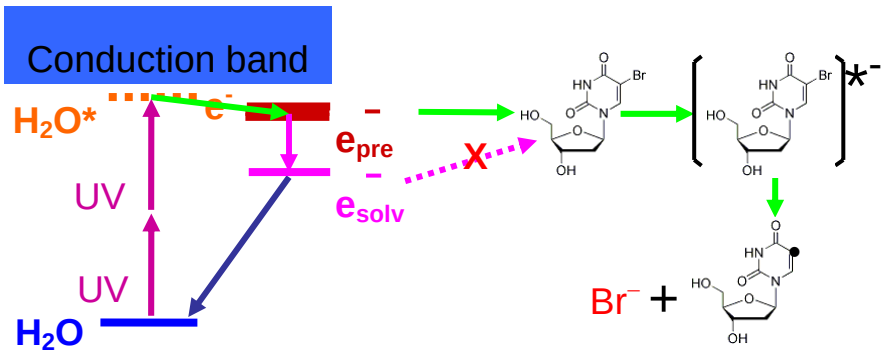

3.1 Introduction

Real-time observation of the transition state in a chemical reaction is of great interest, since it is important to know the properties of the transition state if one is to predict, understand and modify the course of a reaction [1]. The application of time-resolved femtosecond laser spectroscopy to the studies of transition states led to the birth of a new field in chemistry called femtochemistry [2], which has quickly developed into another new field called femtobiology in the past decade. Electron transfer (ET) underlies many reactions in chemical, biological, physical and environmental systems [3-8].

Replacement of thymidine in DNA by halopyrimidines such as bromodeoxyuridine (BrdU, **Scheme 1**) and iododeoxyuridine (IdU) has long been known to enhance DNA damage and cell death induced by ionizing radiolysis and UV photolysis [9-13]. Moreover, halopyrimidines have also been exploited to probe protein-nucleic acid interactions and nucleic acid structure via inducing DNA/RNA-protein photocrosslinking [14-16]. Identified as a potential sensitizer for radiotherapy of cancer, BrdU has been tested in several Phase I - Phase III clinical trials [17-19]. Generally the clinical results have not been satisfactory and therefore BrdU has not been approved for clinical use. This is probably due to poor understanding of the mechanism of the radio-/photosensitivity enhancement [20]. It is generally believed that the first and critical step involved in the action of BrdU is the dissociative electron attachment (DEA) to BrdU, leading to the formation of an anion and a highly reactive radical $dU^{\bullet}$: $e^- + BrdU \rightarrow BrdU^{*-} \rightarrow Br^- + dU^{\bullet}$ [20, 21]. This seems reasonable, since halogen (chlorine, bromine and iodine) containing molecules are well known to have extremely large DEA cross sections at electron energies near zero eV, as seen by Abdoul-Carime et al. [22]. However, the origin and the nature of the electron responsible for this ET reaction in

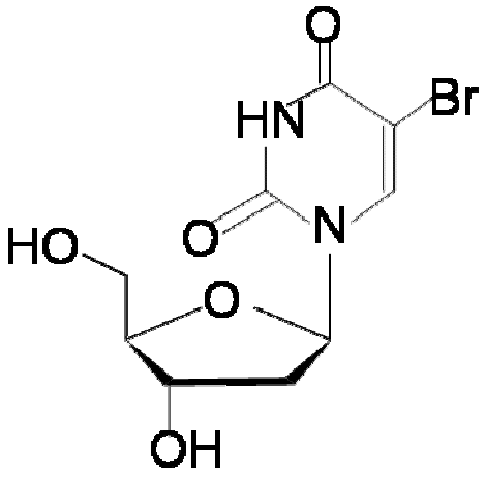

Scheme 1. Chemical structure of BrdU

radio-/photosensitization of BrdU are not well known, and different mechanisms were proposed in the literature. In UV sensitization with BrdU, it was suggested that the reaction involves an ET from a neighboring DNA base (adenine) [11-13], while in radiosensitization it was proposed that the electron involved in the ET reaction is a solvated (hydrated) electron (e_{hyd}^-) as a result of radiolysis of water in biological environments during ionizing radiation [20, 21].

The hydrated electron (e_{hyd}^-), having an absorption band in the visible light peaking at 720 nm, is a well-known product in ionizing radiation of a biological system; a great deal of information is known about the hydrated electron and its chemistry [23]. It is generally accepted that the hydrated electron is responsible for bond breaking in halogen (Cl, Br or I)-containing compounds to form halogen ions. With the advent of time-resolved femtosecond laser spectroscopy, however, the solvation (hydration) dynamics of an excess electron, e.g., produced via two-UV-photon excitation in water, has been studied in certain details [24-27]. As shown in Figure 3.1, electron solvation is now known to occur essentially through two major stages: before becoming fully solvated, the electron is localized in a weakly-bound preexisting trap and is called a precursor to the hydrated electron, denoted as e_{pre}^- hereafter, with a lifetime <1 ps [24-27]. A more recent study by Laenen et al. [28] has shown evidence for multiple precursor states with lifetimes of 110 fs, 200 fs and 540 fs, respectively, which have absorption in the wavelength range from NIR to IR (μm). It has been proposed that e_{pre}^- is responsible for the large enhancements in electron-induced bond breaking of halogenated molecules such as chlorofluorocarbons (CFCs, environmentally important ozone-depleting substances) adsorbed on water ice, which is relevant to the formation of the ozone hole in earth's atmosphere [29-32]. This is probably related to the fact that the weakly-bound e_{pre}^- has energies close to the DEA resonance energies of halogen (Cl, Br

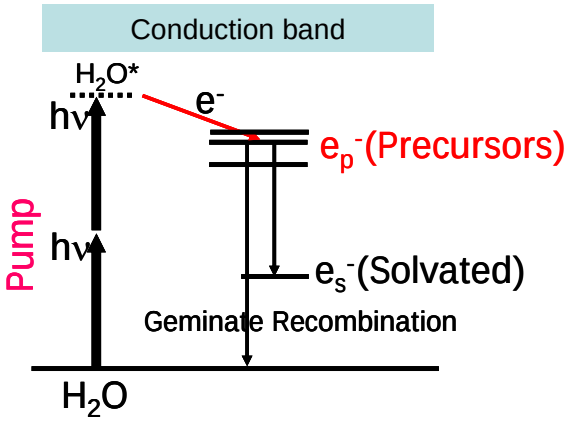

Figure 3.1. Femtosecond salvation dynamics of electrons in water.

and I)-containing molecules near zero eV. However, the role of prehydrated electrons on electron-driven processes involving molecules in aqueous environments is generally poor understood and is relevant to several critical issues facing environmental scientists and radiation biologists (see, e.g., a recent review in ref. 8). Direct observation of the ET between e_{pre}^- and halogenated molecules is thus of great interest; it has been difficult and not yet been obtained, because of the ultrashort lifetimes of e_{pre}^-, on the femtosecond time scale. Previous nanosecond (ns) pulse radiolysis experiments on BrU showed a transient absorption peak at ~330 nm, which was attributed to the transition state BrU^{*-} [21]. But without a fs resolution it was impossible to observe the formation of the real transition state and therefore to determine which species, whether e_{pre}^- or e_{hyd}^-, leads to the reaction. Using fs-resolved laser spectroscopy, Lu et al. [33] recently investigated the possible reaction of e_{pre}^- with BrdU. In those experiments, a reduction the e_{pre}^- signal was initially observed, but it was due to the absorption of the 266 nm pump pulse by BrdU. BrdU absorption has peaks at 267 nm and 279 nm and extends up to 315 nm. At low BrdU concentrations, any *true* reduction in the e_{pre}^- signal would indicate *ultrafast long-range* electron transfer [33]. After avoiding the direct absorption by BrdU, the results showed no such a reduction in the electron signal and thus no such a long-range ET reaction. However, it is still possible to observe the *short-range* reaction of e_{pre}^- with BrdU by directly detecting the formation of the transition state, $BrdU^{*-}$. Herein, we report the first real-time observation of *the transition state* of the ultrafast ET reaction of BrdU with the precursor electron (e_{pre}^-).

3.2 Experimental details

The methodology for pump-probe femtosecond transient absorption measurements in the Waterloo's laboratory is similar to that was described previously (6, 29). We used a Ti:sapphire laser system producing 120 fs, 1mJ laser pulses centered at λ=800 nm at a repetition rate of 1 kHz, two optical parametric amplifiers producing pump and probe pulses with wavelengths from visible to infrared. Alternatively, a femtosecond tripler was used to produce a 266 nm pulse. The polarization of pump and probe pulses was set at the magic angle (54.7°) to avoid contribution from polarization anisotropy due to orientation motions of molecules. A small pump pulse energy (≤0.3 μJ) was used to make the solvated electron signal negligible when detected at (probe) wavelengths around 330 nm and to avoid any nonlinear effects. The sample was held in a 5 mm cell with a stirring bar to avoid any photoproduct accumulation. Ultrapure water with a resistivity of > 18 MΩ/cm was used and BrdU from Sigma-Aldrich was used as supplied. The purity / concentrations of BrdU were checked / calibrated by static absorption spectra of the BrdU, measured with a UV/Visible/NIR spectrophotometer (Beckman, life sciences).

3.3 Results and discussion

Figure3.2 is a plot of the measured static absorption spectrum of a fresh sample of 0.44 mM BrdU in water in a 5-mm quartz cell; the concentration calibration curve was obtained with our measurement of the BrdU extinction coefficient (α=8790 $M^{-1}cm^{-1}$ at 279.5 nm) .

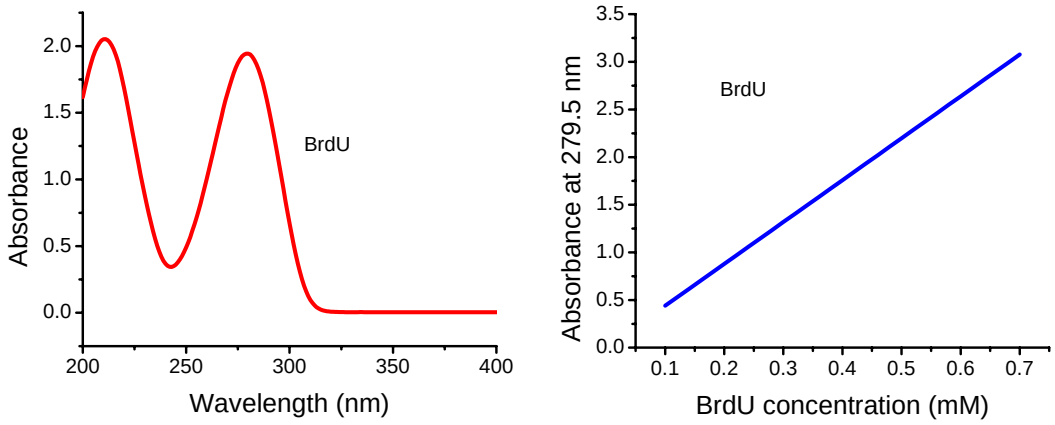

Figure 3.2. (Left) Static absorption spectrum of 0.44 mM BrdU in water; (Right) The absorbance at 279.5 nm as a function of BrdU concentration in a 5-mm cell.

Our pump-probe fs-resolved experiments were first conducted with the excitation (pump) wavelength at 266 nm and the detection (probe) at 330 nm to measure the transition species $BrdU^{*-}$. With λ_{pump}=266-320 nm, the 2-photon excitation mechanism for electron generation in water was verified by the measured quadratic dependence of the transient absorption intensity of e_{pre}^- / e_{solv}^- on the pump power. For BrdU solutions, a strong signal in the transient absorption spectrum is indeed observed, as shown in Figure 3.3. However, the decay of the signal is quite rapid on a subpicosecond scale and superposes on a slow component. The best fit to the data gives three lifetimes: a rapid decay with τ_1 = 0.4±0.1 ps, a long tail with τ_3 in ns, and an immediate τ_2 with a larger uncertainty. Measuring the spectra carefully with varying the pump power, we observe that the intensity of the signal peak at 0.2 ps does not show a quadratic but a linear dependence on the pump power (the inset in Figure 3.3), while the absorbance in the long tail does show a quadratic dependence. This indicates that at least two species contribute to the signal and the rapidly decaying signal results from one single photon process and not from the electron generated by the two-photon excitation process. Therefore the rapidly decaying species cannot be due to the transition state $BrdU^{*-}$. Moreover, there is essentially no rising time in the signal considering the total instrument response

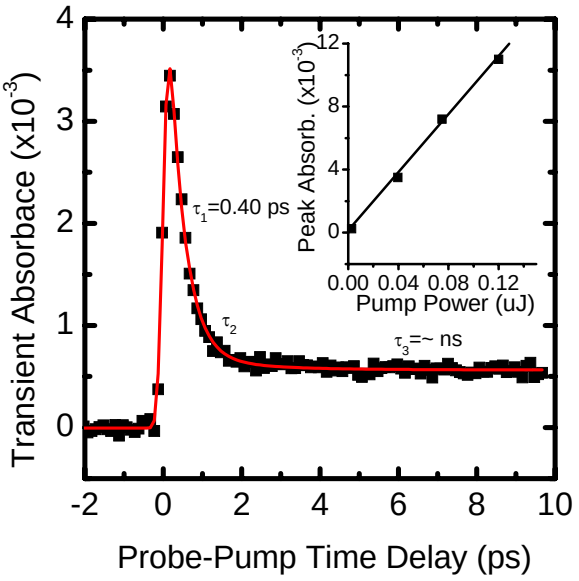

Figure 3.3. Femtosecond transient absorption spectrum of 5 mM BrdU in water, pumped at 266 nm and probed at 330 nm. The solid line is the best fit to the experimental data (solid squares). The inset is the peak absorption at 0.2 ps as a function of pump power.

function of 0.2-0.4 ps [33]. This fast component can be explained as due to the excited state BrdU* resulted from the absorption of 266 nm photons by BrdU [33]. It is therefore most likely that the rapidly decaying species is the BrdU* that has also strong absorption at 330 nm, while the signal associated with the transition state $BrdU^{*-}$ is weaker because of its involvement of the two-photon excitation and is buried in the stronger BrdU* signal.

To avoid the absorption by BrdU, we varied the pump pulse wavelength λ_{pump} to 318 nm while keeping the probe pulse wavelength λ_{probe} at 330 nm. The results are plotted in Figure 3.4a. Since the wavelengths of the pump and probe pulses are now close to each other, a coherent 'spike' appears at the time zero, which is most clearly seen in the spectrum for the pure water. The 'spike' shape depends sensitively on the overlapping geometry and the focusing of the pump and the probe beam. For wavelengths ≥315 nm, the absorption of BrdU is negligible, as seen in the UV-vis spectrum [33]. The result now shows that the rapidly decaying species due to BrdU* disappears in the spectra and there is a clear rising in the signal that peaks at ~0.55 ps. The transient absorption spectra simply exhibit a linear dependence on BrdU concentration in the measured range of 0.1 to 31 mM. This indicates that the transient absorption signal does result from the BrdU molecules. By subtracting the transient absorption spectrum for the pure water from those of BrdU, the 'spike' can be removed nearly completely from the spectra, as

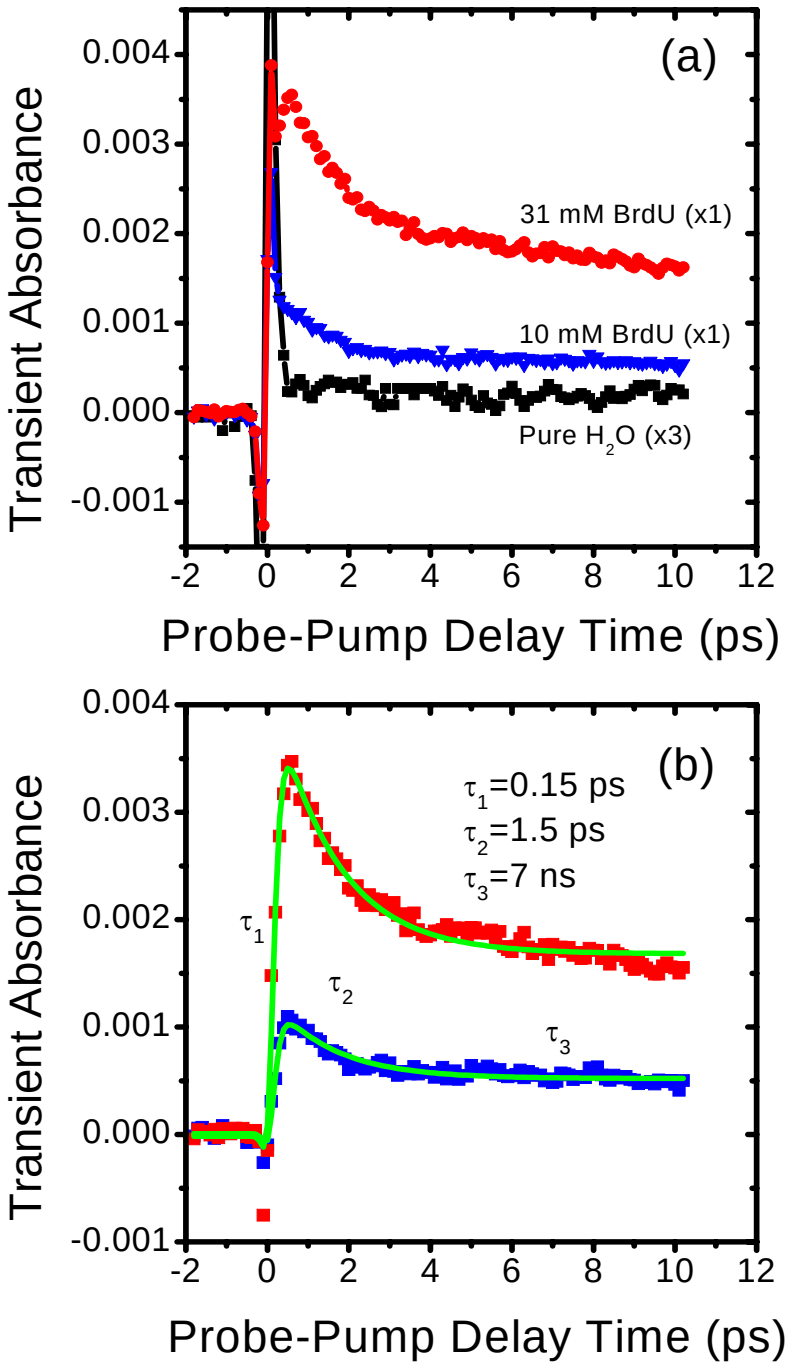

Figure 3.4. Femtosecond transient absorption spectra of BrdU in water, pumped at 318 nm and probed at 330 nm: (a) original data, where the sharp peak at time zero is the coherence "spike" observed when λ_{pump} and λ_{probe} are close to each other; (b) spectra obtained after the subtraction of the spectrum for the pure water. The solid lines in (b) are the best fit to the experimental data, giving a rising time τ_1=0.15 ps and two decay times shown in Figure 3.4b.

shown in Fig. 3.4b. This subtraction makes it possible to make a theoretical fit to the experimental spectra, and hence the formation and decay times of the transient species can be quantitatively obtained. From the fits using Eq. (2.2) in Chapter 2, we obtain a formation time of ~150±50 fs and two decay times: one is of ~1.5±0.3 ps and the other in the scale of ns. The ns decaying component seems consistent with the result observed in previous ns pulse radiolysis experiments [21]. Moreover, the yield of the transient absorption at 330 nm now shows a quadratic dependence on the pump pulse energy, as shown Figure 3.5. The possibility to attribute this transient absorption to the BrdU** state produced via 2-photon excitation of BrdU can be ruled out by the observation that no transient absorption signal can be detected as the pump wavelength is ≥400 nm, while the 2-photon excitation cross section of BrdU has maxima at 534 nm and 558 nm [33]. These results indicate that the transient species detected in the present experiments must originate from the electrons generated via two-photon excitation of H_2O molecules. Furthermore, the transient absorption spectra were also measured with varying probe wavelengths while keeping λ_{pump} at 318 nm. The results are plotted in Figure 3.6, showing that the transient species has indeed an absorption peak at 330 nm. This observation of the absorption peak similar to that detected in ns resolved radiolysis demonstrates that the transient species observed in ns resolved experiments evolves from the short-lived species revealed in current fs experiments.

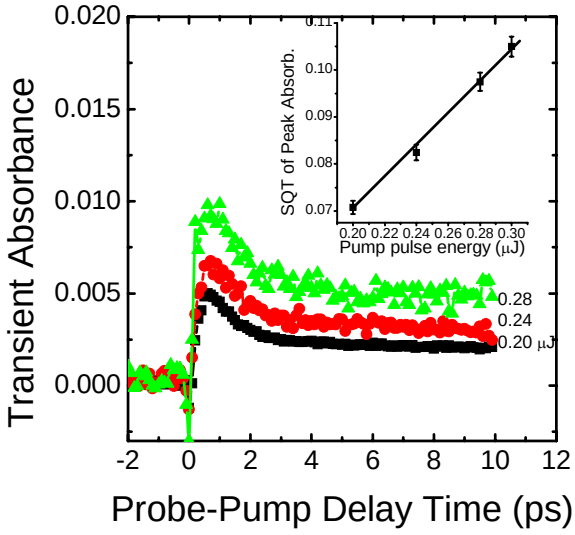

Figure 3.5. Femtosecond transient absorption spectra of 10 mM BrdU in water, pumped at 318nm with various pulse energies and probed at 330nm, after the subtraction of the spectrum for the pure water. The inset is the square root (SQR) of the absorbance peak intensity at 0.55 ps versus pump pulse energy.

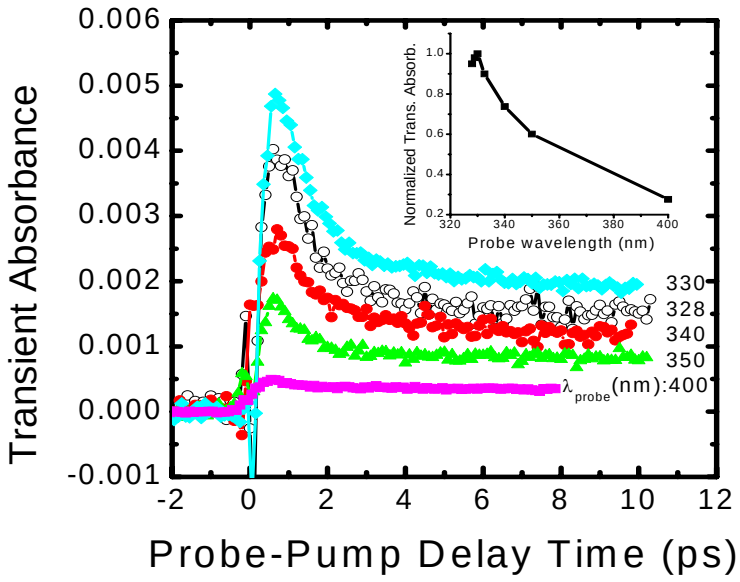

Figure 3.6. Femtosecond transient absorption spectra of 10 mM BrdU in water, pumped at 318 nm and probed at various wavelengths, after the subtraction of the spectrum for the pure water. The inset is the normalized peak transient absorbance A at 0.55 ps versus probe wavelength, where A=[A(0.55 ps)-A(8ps)]/A(8ps).

One might also consider the possibility that the time-resolved transient absorption spectra peaking at ~0.55 ps shown in Figures 3.4-3.6 be due to the signal of the solvated electrons that might be generated by BrdU. However, this speculation is clearly inconsistent with the following facts. *First*, BrdU is a well-known strong electron scavenger under either ionizing or UV radiation and is therefore explored as a radio-/photo-sensitizer [9-13]. *Second*, BrdU have no considerable absorption at 320 nm (see Figure 3.2) and thus there is no basis for BrdU to produce electrons. *Third,* the transient absorption spectra for BrdU shown in Figures 3.4-3.6 are drastically different from that for solvated electrons, whose signal is negligibly small for probe wavelengths ≤350 nm but detectable with an extremely low noise level in the spectrum (as magnified by 3 times in Figure 3.4a). The signal of e_{solv}^- detectable at various visible wavelengths shows a slow rising time of about 1 ps and almost no decay in the first two ps, reported widely in refs. 24-28 and ref. 33 and repeated in Figure 3.4a. *Fourth*, e_{solv}^- has a light absorption peak at ~720 nm [23], which differs drastically from the observed absorption peak at 330 nm for the transient species associated with BrdU (Figure 3.6). These facts and results lead to a conclusion that the transient absorption peaking at 330 nm must be attributed to the transition species $BrdU^{*-}$, neither to the BrdU* / BrdU** /$BrdU^+$ nor to e_{solv}^-.

The present fs-resolved results reveal novel features of the formation and decay of $BrdU^{*-}$. First, the present results demonstrate that $BrdU^{*-}$ forms rapidly within 200 fs after the electronic excitation. Second, the ns-resolved experiments suggested that the transient species would have a lifetime of ~7.0 ns [21]. Generally, however, DEA takes place in a time scale close to the vibration period of a molecule, which lies in the range of 10^{-12} s (ps) to 10^{-15} s (fs) among molecules. Beyond this, the transition state of the molecule either has dissociated into fragments or has relaxed into a nondissociative anionic state. Indeed, the lifetimes of transient (AB^{*-}) states of many halogenated molecules (ABs) are measured to be in the range of 0.1 to several ps [34]. Thus, it is reasonable to assign the faster decay of 1.5±0.3 ps to the dissociation of $BrdU^{*-}$ into Br^- and $dU^{\bullet}$. It is not surprising that the ns resolved experiments could not reveal the rapid formation and the fast decay in the time scales from fs to ps of the transient state.

The ns slow decaying can be attributed to the relaxed, nondissociative $BrdU^-$ following the dissipation of the vibrational energy in $BrdU^{*-}$. We have confirmed the above assignments of the faster decay of 1.5±0.3 ps to the dissociation of $BrdU^{*-}$ into Br^- and $dU^{\bullet}$ and of the ns slow decay to the nondissociative $BrdU^-$ state by conducting similar measurements with another halopyrimidine FdU. The results to be shown in next Chapter shows that no signal for the transition state of a 1.5 ps decay time but only a weak ns-decay signal (FdU^-) is observed for FdU, in good agreement with the fact that the electron attachment to FdU is endothermic and no dissociation occurs for attachment of electrons with energies ≤ 3.0 eV [22], certainly for the weekly bound precursor electrons (below zero eV).

The present observation of the rapid formation of $BrdU^{*-}$ on a time scale of ≤0.2 ps is of particular significance, which clearly demonstrates that this transition species does not result from the fully solvated, well-bound electron (e_{solv}^-), which would be generated in later stages ≥1.0 ps. Only can the precursor electron, e_{pre}^-, result in the formation of the transient species in such a short period of time following the electronic excitation. In other words, the present results provide a direct observation of the ultrafast electron transfer reaction involving e_{pre}^-, that leads to the formation of the transient $BrdU^{*-}$.

3.4 Conclusions

In summary, we report the first real-time observation of *the transition state* of the ultrafast ET reaction of the precursor to the hydrated electron with a biologically important halogenated molecule, BrdU as a radio- and photo-sensitizer in cancer therapy. Our time-resolved fs laser spectroscopic results show that the ET reaction with BrdU is completed within ~0.2 ps after the electronic excitation event, which clearly shows that it

is e_{pre}^-, rather than e_{solv}^-, that leads to the reaction. The mechanism revealed here, an ultrafast ET followed by dissociative electron attachment of the precursor electron to BrdU (e_{pre}^- + BrdU $\rightarrow$ BrdU*$^-$ $\rightarrow$ Br^- + $dU^{\bullet}$), will work for not only the radiosensitization but the photosensitization of BrdU, since e_{pre}^- is a universal product in both ionizing and UV photon radiation. Moreover, the significance of the present results can be extended to understanding of the role of water in electron-initiated processes of molecules in aqueous environments and the subsequent radical chemistry, which is significant in such diverse fields as stratospheric ozone depletion, waster remediation and environmental cleanup, nuclear reactors, radiation processing and medical diagnosis and therapy [8]. As the present results show, nonequilibrium precursor electrons may play a far-reaching role in electron-initiated reactions in many biological and environmental systems.

References:

1. J. C. Polanyi, and A. H. Zewail, "Direct Observation of the Transition State", Acc. Chem. Res. **28**, 119(1995).
2. A. H. Zewail, "Femtochemistry: Atomic-Scale Dynamics of the Chemical Bond Using Ultrafast Lasers (*Nobel Lecture*)", Angew. Chem. Int. Ed. **39**, 2586(2000).
3. G. J. Kavarnos, and N. J. Turro, "Photosensitization by reversible electron transfer: Theories, experimental evidence, and examples", Chem. Rev. **86**, 401(1986).
4. R. A. Marcus, "Electron Transfer Reactions in Chemistry: Theory and Experiment (Nobel Lecture)", Angew. Chem. Int. Ed. **32**, 1111(1993**).**
5. C. J. Murphy, M. R. Arkin, Y. Jenkins, N. D. Ghatlia, S. H. Bossmann, N. J. Turro, and J. K. Barton, "Long-Range Photoinduced Electron Transfer Through a DNA Helix", Science **262**, 1025(1993).
6. C. Wan, T. Fiebig, S. O. Kelley, C. R. Treadway, J. K. Barton, and A. H. Zewail, "Femtosecond dynamics of DNA mediated electron transfer", Proc. Natl. Acad. Sci. **96**, 6014(1999).
7. X. Qu, C. Wan, H.-C. Becker, D. Zhong, and A. H. Zewail, Proc. Natl. Acad. Sci. "The anticancer drug-DNA complex: Femtosecond primary dynamics for anthracycline antibiotics function", **98**, 14212(2001).
8. B.C. Garrett, et al., "Role of water in electron-initiated processes and radical chemistry: Issues and scientific advances", Chem. Rev. **105**, 355(2005).
9. W. C. Dewey, B. A. Sedita, and R. M. Humphrey, "Radiosensitization of X chromosome of Chinese Hamster cells related to incorporation of 5-Bromodeoxyuridine", Science **152**, 519(1966**)**.
10. F. Q. Hutchinson, Rev. Biophys. **6**, 201(1973).

11. H. Sugiyama, Y. Tsutsumi, and I. Saito, “Highly sequence-selective photoreaction of 5-Bromouracil containing deoxyhexanucleotides”, J. Am. Chem. Soc. **112**, 6720(1990).
12. G. P. Cook, and M. M. Greenberg, “A novel mechanism for the formation of direct strand breaks upon anaerobic photolysis of duplex DNA containing 5-Bromodeoxyuridine”, J. Am. Chem. Soc. **118**, 10025(1996).
13. T. Chen, G. P. Cook, A. T. Koppisch and M. M. Greenberg, “Investigation of the origin of the sequence selectivity for the 5-halo-2’-deoxyuridine sensitization of DNA to damage by UV-irradiation”, J. Am. Chem. Soc. **122**, 3861(2000).
14. E. E. Blatter, Y. W. Ebright, and R. H. Ebright, “Identification of an amino acid-base contact in the GCN4-DNA complex by bromouracil mediated photocrosslinking”, Nature (London) **359**, 650(1992).
15. M. C. Willis, B. J. Hicke, O. C. Uhlenbeck, T. R. Cech, and T. H. Koch, “Photocrosslinking of 5-iodouracil substituted RNA and DNA to proteins”, Science **262**, 1255(1993).
16. B. J. Hicke, M. C. Willis, T. H. Koch, and T. R Cech, “Telomeric protein-DNA point contacts identified by photo-crosslingking using 5-Bromodeoxyuridine”, Biochemistry **33**, 3364(1994).
17. M. D. Prados, et al. “A phase 3 randomized study of radiotherapy plus procarbazine, CCNU, and vincristine (PCV) with or without BUdR for the treatment of anaplastic astrocytoma: a preliminary report for RTOG 9404”, Int. J. Radiat. Oncol. Biol. Phys. **45**, 1109(1999).
18. J.-P. Pignol, E. Rakovitch, D. Beachey, and C. Le Sech, “Clinical significance of atomic inner shell ionization (ISI) and Auger cascade for radiosensitization using IUdR, BUdR, platinum salts, or gadolinium porphyrin compounds”, Int. J. Radiat. Oncol. Biol. Phys. **55**, 1082(2003).
19. Y. Li, A. Owusu, and S. Hehnert, “Treatment of intracranial rat glioma model with implant of radiosensitizer and biomodulator drug combined with external beam radiotherapy”, Int. J. Radiat. Oncol. Biol. Phys. **58**, 519(2004).
20. S. Cecchini, S. Girouard, M. A. Huels, L. Sanche, and D. J. Hunting, “Interstrand cross-links: a new type of γ ray damage in Bromodeoxyuridine substituted DNA”, Biochemistry **44**, 1932(2005).
21. E. Rivera, and R. H. Schuler, “Intermediates in the reduction of 5-halouracils by e_{aq}^-”, J. Phys. Chem. **87**, 3966(1983).
22. H. Abdoul-Carime, M. A. Huels, F. Bruning, E. Illenberger, and L. Sanche, J. “Dissociative electron attachment to gas-phase 5-bromouracil”, J. Chem. Phys. **113**, 2517(2000); H. Abdoul-Carime, M. A. Huels, E. Illenberger, and L. Sanche, J. Am. Chem. Soc. **123**, 5354 (2001).
23. E. J. Hart, and M. Anbar, “The Hydrated Electron” (Wiley-Interscience, New York, 1970).

24. A. Migus, Y. Gauduel, J. L. Martin, and A. Antonetti, "Excess electrons in liquid water: First evidence of a prehydrated state with femtosecond lifetime", Phys. Rev. Lett. **58**, 1559(1987).
25. F. H. Long, H. Lu, and K. B. Eisenthal, "Femtosecond studies of the presolvated electron: An excited state of the solvated electron?", Phys. Rev. Lett. **64**, 1469(1990).
26. T. Goulet, A. Bernas, C. Ferradini, and J.-P. Jay-Gerin, "On the electronic structure of liquid water: Conduction-band tail revealed by photoionization data", Chem. Phys. Lett. **170**, 492(1990).
27. A. Bernas, C. Ferradini, and J.-P. Jay-Gerin, "On the electronic structure of liquid water: Facts and reflections", Chem. Phys. **222**, 151(1997).
28. R. Laenen, T. Roth and A. Laubereau, "Novel Precursors of Solvated Electrons in Water: Evidence for a Charge Transfer Process", Phys. Rev. Lett. **85**, 50(2000).
29. Q.-B. Lu, and L. Sanche, "Effects of Cosmic Rays on Atmospheric Chlorofluorocarbon Dissociation and Ozone Depletion", Phys. Rev. Lett. **87**, 078501(2001).
30. Q.-B. Lu, and L. Sanche, "Enhanced Dissociative Electron Attachment to CF_2Cl_2 by Transfer of Electrons Localized in Preexisting Traps of Water and Ammonia Ice", Phys. Rev. B**63**, 153403(2001).
31. Q.-B. Lu, and L. Sanche, "Large Enhancement in Dissociative Electron Attachment to HCl adsorbed on H_2O Ice via Transfer of Presolvated Electrons", J. Chem. Phys. **115**, 5711(2001).
32. Q.-B. Lu, and L. Sanche, "Dissociative Electron Attachment to CF4, CFCs and HCFCs adsorbed on H_2O Ice", J. Chem. Phys. **120**, 2434(2004).
33. Q.-B. Lu, J. S. Baskin, and A. H. Zewail, "The Presolvated Electron in Water: Can It Be Scavenged at Long Range?", J. Phys. Chem. B**108**, 10509(2004)**.**
34. C. D. Finch, R. Parthasarathy, H. C. Akpati, P. Nordlander, and F. B. Dunning, "Low-energy dissociative electron attachment to $CFCl_3$, CF_2Br_2, and 1,1,1- and 1,1,2-$C_2Cl_3F_3$: Intermediate lifetimes and decay energetics", J. Chem. Phys. **106**, 9594(1997).

Chapter 4

Molecular Reaction Mechanism of Halopyrimidines as Radiosensitizing Drugs and the Physical Nature of the Prehydrated Electron in Water

Table of Contents Graphic

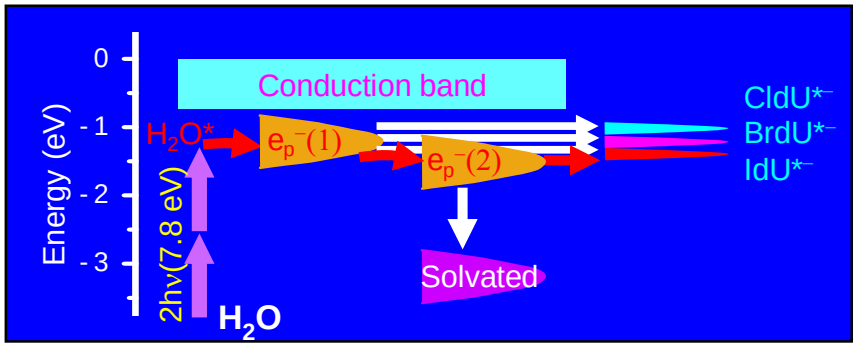

4.1 Introduction

As described in last Chapter, our time-resolved femtosecond laser spectroscopic study of the molecular reaction mechanism of BrdU as a radiosensitizing drug has revealed that it is the ultrafast electron transfer (UET) reaction of BrdU with a short-lived, weakly-bound precursor electron (e_{pre}^-), rather than with the deeply-trapped (well-bound) hydrated electron (e_{hyd}^-), that is responsible for the radical formation from BrdU [1]. In the present work, we extend this study to all four potential radiosensitizers XdUs (X=F, Cl, Br and I). In gas-phase experiments, Abdoul-Carime et al. [2] have found that halouracils (XUs) have extremely large dissociative electron attachment (DEA) cross sections at thermal electron energies near zero eV. However, they showed that the efficiency for the uracilyl radical formation by DEA of 0-3 eV electrons is in the order of BrU>ClU>IU, while the efficiency for the halogen atomic radical is ClU>BrU>IU, thus concluding that ClU should be the most effective radiosensitizer among halouracils. This conclusion seems inconsistent with the observations of the biological and therapeutic effects of halopyrimidines, which have so far shown that only IdU and BrdU are the most effective radiosensitizers [3-14], and with the theoretical calculations by Li et al. [15, 16] that have showed the DEA efficiency of BrU≥ClU>>FU.

Moreover, halopyrimidines (particularly IdU, Scheme 1) will be employed as quantum-state-specific molecular probes to reveal the lifetimes and physical nature of the non-equilibrium precursors to the hydrated electron. Since the advent of fs laser spectroscopy in the late 1980s, the existence of e_{pre}^- in bulk water or water clusters has been studied both experimentally and theoretically [17-33]. In bulk water, the hydrated electron e_s^- is believed to be confined in a small cavity and to occupy a s-like ground state at ~–3.2 eV from the vacuum level [17, 23, 30]. The absorption of e_s^- peaks at 1.7

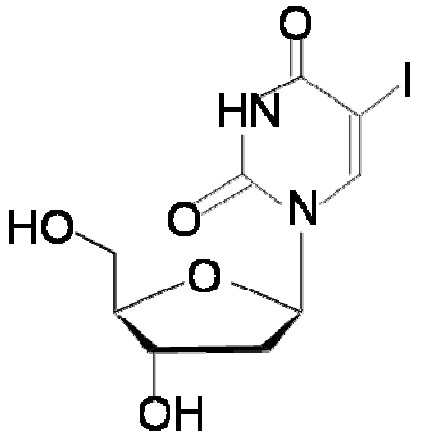

Scheme 1. Chemical Structure of IdU

eV (~720 nm) and can be thought of as a transition from the ground state to a p-like excited state at ~–1.5 eV, in analogy to the electronic structure of a hydrogen atom [23, 30]. Quantum molecular dynamics (MD) simulations by Rossky and co-workers [19] have concluded that e_{pre}^- is a p-like excited state and has a lifetime of ~1.0 picosecond (ps) (1ps=10^{-12} s). Jay-Gerin and co-workers [21, 22] have proposed that e_{pre}^- is an electron localized at a preexisting trap related to the Urbach tail extending below the water conduction band. Fs laser spectroscopic studies have reported various e_{pre}^- lifetimes of 50 fs, ~200 fs, ~540 fs and ~1 ps [18, 20, 24-29]. In particular, Long et al. [20] have observed a two-state model with lifetimes of 180 fs and 540 fs for the precursors. Laenen et al. [25, 26] have shown clear evidence for the existence of consecutive precursor states with lifetimes of 110 fs, 200 fs and 540 fs, respectively, which have absorption peaks at 2900 nm, 1600 nm and ~900 nm, following two-UV-photon excitation of H_2O. Kambhampati et al. [27] have also shown the existence of various precursor states of ~50 fs, 200~300 fs and 400 fs depending on the initial state of the electron in water. Long et al. [20] attributed the e_{pre}^- of a 540 fs lifetime to the so-called wet electron that is really an electronically excited state of e_{hyd}^-, consistent with the theoretical prediction by Rossky and co-workers [19]. In contrast, Laenen et al. [26] attributed both the "wet electron" of a 540 fs lifetime and the e_{pre}^- of a ~200 fs lifetime to the (s-like) ground-state electrons embedded in hot solvation shells. Kambhampati et al. [27] attributed the 200 fs to be the lifetime of the e_{pre}^- electron located in preexisting traps in water after two UV photon excitation of water. Also, Kambhampati et al. [27] and Pshenichnikov et al. [28] have attributed the lifetime of ~50 fs to the p-excited state of the hydrated electron and all the precursors with lifetimes longer than 50 fs to the s-like ground state in their three-pulse experiments. In latter experiments, the hydrated electron was first prepared by a high intensity UV pulse followed by pump-probe detection of the excited-state dynamics of the hydrated electron. The attribution of the 50 fs process to the lifetime of the p-excited state seems to be supported by some recent *anionic water cluster* experiments [31, 32]. However it is still an open question as to whether the cluster observations can be extended to the bulk properties of liquid water [33]. From the above facts, it is reasonable to conclude that there have been significant controversies about the physical natures of the e_{pre}^- states in water.

4.2 Experimental details

The standard methodology for pump-probe fs transient absorption measurements has been described in Chapter 2. We used a Ti:sapphire laser system producing 120 fs, 1mJ laser pulses centered at λ=800 nm at a repetition rate of 1 kHz, two optical parametric amplifiers producing pump and probe pulses with wavelengths from visible to infrared. The polarization of pump and probe pulses was set at the magic angle (54.7°) to avoid

contribution from polarization anisotropy due to orientation motions of molecules. To avoid the direct absorption of the pump pulse by halopyrimidines, a pump wavelength ≥320 nm was used in these experiments and excess electrons are produced by a two-photon excitation process in water [1, 29]. The probe wavelengths around 330 nm were selected to search the transition states (XdU^{*-}) of the reactions of e_{pre}^- with XdU (X=F, Cl, Br and I) [1]. A small pump pulse energy (≤100 nJ) was used to make the solvated electron signal negligible when detected at (probe) wavelengths around 330 nm and to avoid any nonlinear effects. Since the pump and probe wavelengths are now close to each other, a coherent 'spike' unavoidably appears at delay time zero, which is clearly seen in the spectrum for the pure water. This "unwanted" spike, however, offers not only a visible and reliable *in-situ* reference for the pump-probe delay time zero but the instrument response function. In our experiments, an instrument response function of 300 fs was directly given by the full width at half maximum (FWHM) of the coherent spike. Transient absorption spectra of XdU^{*-} are corrected by subtracting the spectrum of the pure water from the collected spectra; this also significantly reduces or completely removes the coherence spike from the spectra.

To obtain the precise formation times and the lifetimes of XdU^{*-}, the instrument response function must be taken into account to fit the measured transient absorption spectra. As mentioned in the Introduction, several precursor states to the hydrated electron are known to exist in time sequence for electron hydration in water [18, 20, 24-29]. If two consecutive precursor states react with XdU to form XdU^{*-}, there will be two consecutive contributions to the XdU^{*-} signal, that is, the rising and decay of the XdU^{*-} signal resulting from the second precursor state will occur with a time delay Δt relative to the formation and decay time of the first precursor. Since the formation time of the first precursor is very short, it can approximately be neglected. Thus, $\Delta t \approx \tau_1$, which is the lifetime of the first precursor state, i.e., the first rising time of the XdU^{*-} signal. Then, the time-dependent XdU^{*-} signal is given by,

$$S(t) = S_1(t) + S_2(t - \tau_1). \tag{4.1}$$

Here, $S_1(t)$ and $S_2(t-\tau_1)$ are given by Eq. (2.2) in Chapter 2, respectively. The best fits to the experimental data were obtained by using a least-squares fitting program. In our fits, the time zero and the FWHM (=300 fs) of the pump-probe cross-correlation function are *not* adjustable fitting parameters, but are fixed at the values determined by the coherent spike appearing in the pure water spectrum. This procedure should give rise to more reliable fitted results.

All measurements are conducted at room temperature. The sample was held in a 5 mm cell with a stirring bar to avoid photoproduct accumulation. Ultrapure water with a

resistivity of >18 MΩ/cm was obtained from an ultrapure water system (Barnstead). Halopyrimidines from Sigma-Aldrich were used as supplied and their concentrations are calibrated by taking static absorption spectra from a UV/visible spectrophotometer (Beckman). Except for IdU that has a saturation concentration of ~4.0 mM at 300 K, all BrdU, CldU and FdU have an excellent solubility in water.

4.3 Results

Femtosecond transient absorption spectra of XdUs obtained with λ_{pump}=320 nm and λ_{probe}=330 nm are shown in Figures 4.1a and 4.1b, together with the spectrum for the pure water. The transient absorption spectral intensity as a function of probe wavelength with the same pump wavelength is shown in Figure 4.2. Indeed, the transient absorption exhibits a peak around 330 nm for all XdUs, consistent with the earlier observation for BrdU described in last Chapter and in reference [1]. This result indicates that there

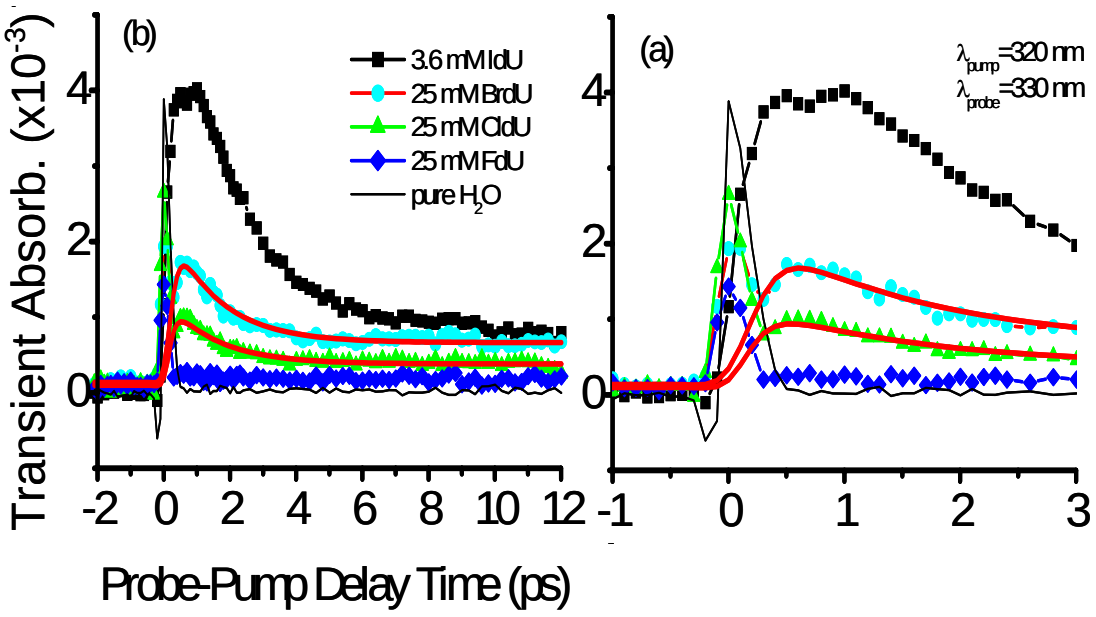

Figure 4.1. Transient absorption spectra of 3.6 mM IdU, 25mM CldU and 25 mM FdU, obtained with the pump and probe wavelengths of 320 nm and 330 nm, respectively, after the subtraction of the spectrum for the pure water, in the delay time ranges of -1 to 3 ps (a) and -2 to 12 ps. The sharp peak at time zero is the coherence "spike" observed when λ_{pump} and λ_{probe} are close to each other. The solid lines in red in the spectra for BrdU and CldU are the best fits to the experimental data, giving a rising time τ_1 = 0.15 ps and two decay times τ_2=1.5 ps and τ_3 in ns.

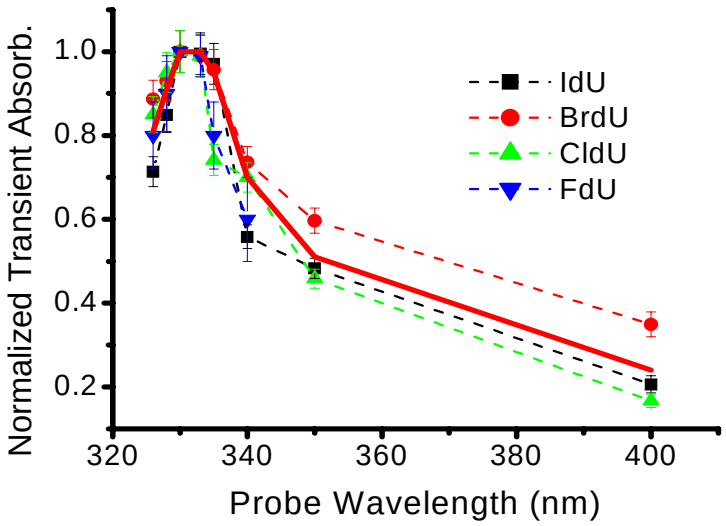

Figure 4.2. Transient absorption intensity of IdU, BrdU, CldU and FdU as a function of probe wavelength in the range of 325 to 400 nm with the pump wavelength fixed at 320 nm. The absorption intensities are normalized to those at the probe wavelength of 330 nm. The solid line in red is an aid to eye.

exists only a single transition state XdU^{*-} of the precursor electron transfer reaction with an XdU. In last Chapter, we have shown that the transient absorption spectra for BrdU have a linear dependence on BrdU concentration in the range of 0.1-30 mM [1]; this linear dependence has now been reconfirmed for other XdUs, as shown in Figure 4.3 for IdU. Thus, higher XdU (X=Br, Cl and F) concentrations were used to obtain the signal intensities comparable with that for IdU in Figure 4.1. The spectrum for FdU exhibits no considerable transient absorption peak in the first ps after the pump excitation, indicating that essentially no DEA of any weakly bound e_{pre}^- to FdU could occur. Instead, only was an extremely weak, flat (long-lived) signal observed for FdU, which can be attributed to the nondissociative molecular anion FdU^-, similar to the long-lived tail observed for BrdU [1]. In contrast, CldU shows a transient absorption spectrum similar to that for BrdU: it exhibits a single signal peak at the delay time of ~0.55 ps with one fast decay time of 1-2 ps superposed on a long-lived (ns), slow decay tail; the transient absorption intensity for CldU is significantly weaker than that for BrdU. The fitted transient absorption spectrum, also shown in Figure 4.1, gives a rising time of ~150 fs, a fast decay time of 1.5 ps and a slow decay time in ns for CldU, corresponding to the formation and the dissociation of $CldU^{*-}$ and the lifetime of the nondissociative $CldU^-$.

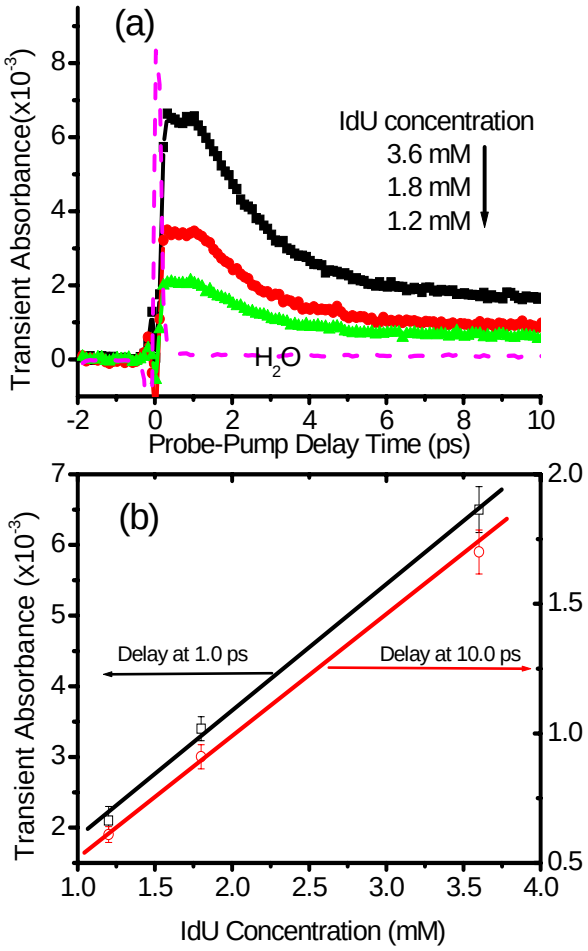

Figure 4.3 (a) Femtosecond time-resolved transient absorption spectra of IdU with various concentrations, probed at 330 nm; the dash line is the spectrum for the pure water; (b) Transient absorption intensities at 1.0 ps and 10.0 ps versus IdU concentration.

These results are nearly identical to those for BrdU, described in last chapter and in ref. 1. It follows that the same excited-state precursor contributes to the formation of $BrdU^{*-}$ and $CldU^{*-}$. Most strikingly, the transient absorption signal for IdU is much stronger than for BrdU and CldU even when the concentration of IdU is about one order of magnitude lower. *In other words, the transient absorption signal intensity for IdU is at least one order of magnitude higher than those for CldU and BrdU with an identical concentration.* In addition, beside the first peak at ~0.5 ps, *a second peak is visible at ~1.0 ps in the transient absorption spectrum for IdU.* These results provide clear evidence of two e_{pre}^- states contributing to the formation of IdU^{*-}.

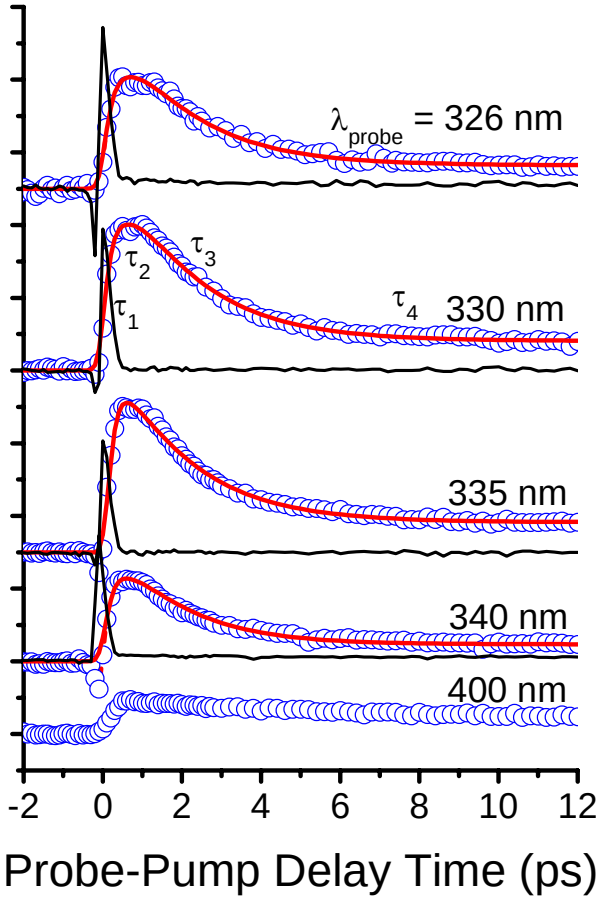

Figure 4.4. Femtosecond transient absorption spectra of 3.6 mM IdU, pumped at 320 nm and probed at various wavelengths. The solid lines in red are the best fits to the time-dependent transient absorption spectra with a model of four-exponential functions which are convoluted with the instrument response function represented by a Gaussian function (see text). The fitted rising and decay times are given in table 1.

Table 4.1. The results given by the best fits to the time-resolved transient absorption spectra with Eq. (4.1): τ_1 and τ_2 are the rising times, while τ_3 and τ_4 are the decay times.

λ_{probe} (nm)	τ_1(fs)	τ_2(fs)	τ_3(ps)	τ_4(ns)
326	240±50	555±50	2.00±0.20	10
330	200±50	540±50	1.90±0.02	10
335	150±50	542±50	1.84±0.02	10
340	140±50	540±50	1.70±0.20	10
Ave.	182±50	544±50	1.86±0.20	10

For the transient absorption spectra measured with probe wavelengths around 330 nm (in the range of 325-335, Figure 4.4), the best theoretical fits always give two rising times and two decay times for each measured spectrum of IdU. The data obtained from the best fits using Eq. (4.1) are given in Table 1. Moreover, the two rising times and two decay times are respectively τ_1=182 ±50 fs, τ_2=544±50 fs, τ_3=1.86 ±0.20 ps and τ_4≈10 ns, with an excellent reproducibility. Similar to the case for BrdU [23] and CldU, the τ_1 rising time, the τ_3 and τ_4 decay times correspond to the lifetime of an precursor e_{pre}^-, the dissociative lifetime of IdU^{*-} and the lifetime of the long-lived molecular anion IdU^-, respectively. Below, our discussion is focused on the rising (formation) times (~0.18 and 0.56 ps) of the transition states XdU^{*-} (X=I, Br and Cl) and the corresponding e_{pre}^- states responsible for their formation.

4.4. Discussion

As mentioned in the Introduction, gas-phase experiments have shown that halouracils (IU, BrU and ClU) have very large cross sections of DEA resonances at thermal electron energies nearly zero eV [2]. The excess energy ΔE for electron-induced C–X (X=I, Br, Cl and F) bond breaks in IdU, BrdU, CldU and IdU in the gas phase can be estimated by $\Delta E = E_A(X) - E_{BD} \equiv \Delta E^0$, where $E_A(X)$ is the electron affinity of the halogen atom X and E_{BD} the C-X bond dissociation energy. In the condensed phase, the excess energy is increased by the polarization energy (E_P) of the medium: $\Delta E = \Delta E^0 + E_P$ [34]. With the ΔE^0 values obtained in the gas phase (ΔE^0 = –0.9 to –1, 0.01, 0.24 and 0.42 eV for FU, ClU, BrU and IU, respectively) [2] and E_p≈1.0 eV for water [35], we estimate that the C–X bond breaks for CldU, BrdU and IdU in water are exothermic by 1.01, 1.24 and 1.42 eV, respectively, while the C–F bond break for FdU in water is nearly thermoneutral (ΔE ≈ 0 eV). As schematically illustrated in Figure 4.5, DEA resonances are therefore expected to occur for CldU and BrdU with the weakly-bound e_{pre}^- states that have energies slightly higher than the p-like excited state of the hydrated electron. For IdU, interestingly, a second DEA channel can additionally occur with the p-like excited state which has a bound energy of ~1.5 eV, very close to the exothermic energy (1.42 eV) for DEA of IdU. In contrast, no precursor states are available for DEA to FdU. Thus, resonant ET from excited-state e_{pre}^- to XdUs is expected to occur efficiently, leading to DEA to IdU, BrdU and CldU with the expected efficiency: IdU>>BrdU>CldU, but no DEA for FdU. This prediction is in good agreement with the observed results.

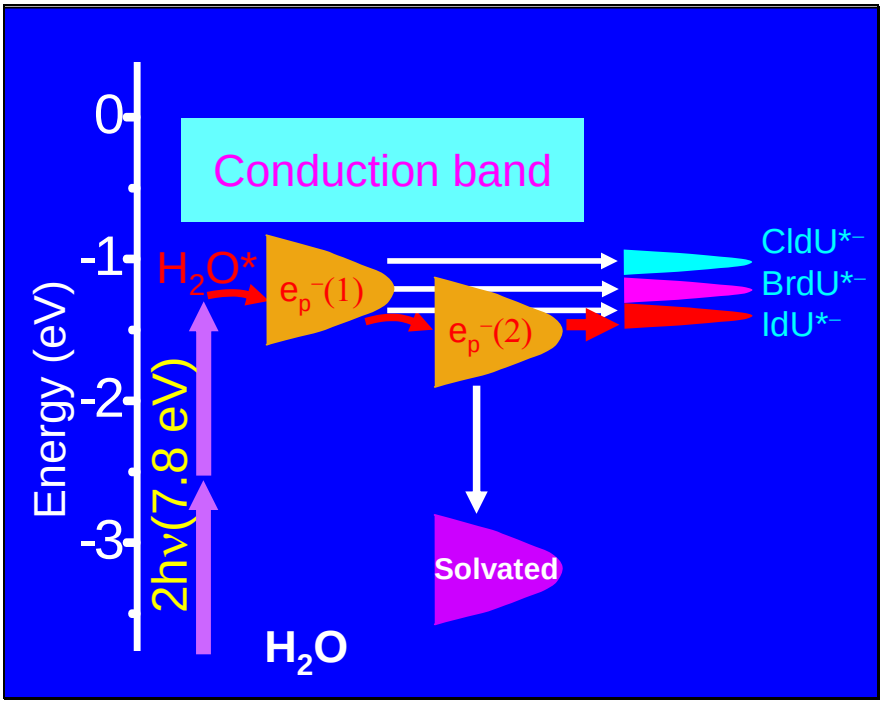

Figure 4.5. Schematic diagram for the energy levels of the equilibrated hydrated electron (e_{solv}^-), the nonequilibrium precursor (prehydrated) states [$e_p^-(1)$ and $e_p^-(2)$] and the dissociative electron attachment (DEA) resonance levels of halopyrimidines (CldU, BrdU and IdU). The s-like ground state and the p-like excited state ($e_p^-(2)$) are located at –3.2 and –1.5 eV, respectively, with respect to the vacuum level. The $e^-:(H_2O)_n$ state, a precursor to the p-like excited state, is denoted as $e_p^-(1)$. The DEA resonance levels, CldU*$^-$, BrdU*$^-$ and IdU*$^-$ are located at the energies of –1.01, –1.24 and –1.42 eV, respectively. The electronic band structure of water is referred to a recent review by Jay-Gerin and co-workers [22], where the band gap between the conduction-band bottom (at ~–0.75 eV) and the valence-band top is estimated to be in the range of 8.2 to 9.2 eV. Thus, in our two 320 nm-photon excitation (7.8 eV), an electron in the water valence band is promoted to an electronic state located at –1.15 to –2.15 eV.

As also shown in Figure 4.5, there are only small differences in the resonance energies for DEA of CldU, BrdU and IdU to form halogen ions and a neutral radical. Actually, the DEA resonant level for IdU is only 0.2 and 0.4 eV below those for BrdU and CldU, respectively. Note that the s-like ground state of e_s^- is located at ~–3.2 eV, which is 1.7 eV below the p-like excited state. As a consequence, it is now clearly revealed that both the first e_{pre}^- with a lifetime of 150~200 fs leading to DEAs of all CldU, BrdU and IdU and the second e_{pre}^- with a lifetime of ~544 fs leading solely to DEA of IdU *must not* be s-like 'hot' or 'cold' electronic ground states, but be electronically excited states of the hydrated electron. According to the electronic structure of liquid water [22], the first excited-state e_{pre}^- subsequent to the two 320 nm-photon excitation (7.8 eV) of water in the present experiments lies in an energy of at most –1.15 eV (–1.15 to –2.15 eV).

Thus, the present results also indicate that the first excited-state e_{pre}^- is very close to the second p-like excited-state e_{pre}^- (at ~−1.5 eV) in energy: both are weakly bound excited states in the energy range of −1.15 to −1.5 eV, highly reactive for ET reactions. In conclusion, the present results provide direct evidence that both e_{pre}^- states with lifetimes of 150~200 fs and ~544 fs are electronically excited states of e_s^-. This also leads to an answer to a long standing debate of whether the "wet electron" with a ~540 fs lifetime is an electronically excited state or a ground state of e_s^-. The absence of these e_{pre}^- states in $(H_2O)_n^-$ clusters [31, 32] may imply that they are related to electrons localized at preexisting traps formed due to the dynamic structure of water.

4.5 Conclusion

We have obtained real-time observations of the reactions of halopyrimidines with precursor electrons generated by ionizing (UV) radiation in water. This study has multiple-fold significance. First, the present results prove that it is the e_{pre}^-, rather than the hydrated electron, that are responsible for the dissociative electron attachment to halopyrimidines. This reaction leads to the formation of the reactive radical, which is a key step in the mechanism of action of these radiosensitizers in radiotherapy of cancers. Our results have challenged a long accepted mechanism that long-lived hydrated electrons would be responsible for the radical formation in radiolysis of halogenated molecules [36] and particularly in radiosensitization of halopyrimidines [13], which would predict a formation time of CldU*$^-$, BrdU*$^-$ and IdU*$^-$ in the time scale beyond ns corresponding to the lifetime of hydrated electrons. Second, we have clearly revealed that the DEA reaction efficiency is IdU>>BrdU>CldU, whereas no DEA reaction of e_{pre}^- with FdU occurs. This is due to the availability of two precursor states for DEA to IdU, of one precursor state for DEAs to BrdU and CldU, and no precursors for DEA to FdU. Thus, *IdU should be explored as the most effective radiosensitizer.* Third, our results reveal the physical nature of the e_{pre}^- states and show direct evidence of the long-sought wet electron in water, where halopyrimides were indeed employed as quantum-state-specific probe molecules. As a more general conclusion, our results demonstrate that despite their ultrashort lifetimes in subpicoseconds, nonequilibrium e_{pre}^- can play a crucial role in many ET reactions occurring in aqueous environments, especially for chlorine-, bromine- and iodine-containing molecules. In summary, this study can have clear significance for understanding of the role of water in electron-initiated reactions and radical chemistry in many chemical, biological and environmental systems, ranging from breakups of environmentally important halogenated molecules [37, 38] to the activation of halogen-containing anticancer drugs [1, 39].

References:

1. C.-R. Wang, A. Hu, and Q.-B. Lu, J. Chem. Phys. **125**, 241102(2006**).**
2. H. Abdoul-Carime, M. A. Huels, E. Illenberger, and L. Sanche, J. Am. Chem. Soc. **123**, 5354 (2001).
3. W. C. Dewey, B. A. Sedita, and R. M. Humphrey, Science **152**, 519(1966).
4. F. Q. Hutchinson, Rev. Biophys. **6,** 201(1973).
5. H. Sugiyama, Y. Tsutsumi, and I. Saito, J. Am. Chem. Soc. **112**, 6720(1990).
6. G. P. Cook, and M. M. Greenberg, J. Am. Chem. Soc. **118**, 10025(1996**)**; T. Chen, G. P. Cook, A. T. Koppisch, and M. M. Greenberg, ibid, **122**, 3861(2000).
7. E. E. Blatter, Y. W. Ebright, and R. H. Ebright, Nature (London) **359**, 650(1992).
8. M. C. Willis, B. J. Hicke, O. C. Uhlenbeck, T. R. Cech, and T. H. Koch, Science, **262**, 1255(1993).
9. J. Hicke, M. C. Willis, T. H. Koch, and T. R. Cech, Biochemistry **33**, 3364(1994).
10. M. D. Prados, et al. Int. J. Radiat. Oncol. Biol. Phys. **45**, 1109(1999).
11. S. Karnas, E. Yu, R. McGarry, and J. Battista, Phys. Med. Biol. **44**, 2537(1999).
12. J.-P. Pignol, E. Rakovitch, D. Beachey, and C. Le Sech, Int. J. Radiat. Oncol. Biol. Phys. **55**, 1082(2003).
13. S. Cecchini, S. Girouard, M. A. Huels, L. Sanche, and D. J. Hunting, Biochemistry **44**, 1932(2005); Radiat. Res. **162**, 604(2004).
14. Y. Li, A.Owusu, and S. Hehnert, Int. J. Radiat. Oncol. Biol. Phys. **58**, 519(2004).
15. X. Li, L. Sanche, and M. D. Sevilla, J. Phys. Chem**.** A **106**, 11248 (2002).
16. X. Li, M. D. Sevilla, and L. Sanche, J. Am. Chem. Soc. **125**, 8916 (2003).
17. K. D. Jordan, Science **306**, 618(2004), and references therein.
18. A. Migus, Y. Gauduel, J. L. Martin, and A. Antonetti, Phys. Rev. Lett. **58**, 1559(1987).
19. P. J. Rossky, and J. Schnitker, J. Phys. Chem. **92**, 4277(1988).
20. F. H. Long, H. Lu, and K. B. Eisenthal, Phys. Rev. Lett. **64**, 1469(1990).
21. T. Goulet, A. Bernas, C. Ferradini, and J.-P. Jay-Gerin, Chem. Phys. Lett. **170**, 492(1990).
22. A. Bernas, C. Ferradini, and J.-P. Jay-Gerin, Chem. Phys. **222**, 151(1997).
23. J. V. Coe, G. H. Lee, J. G. Eaton, S. T. Arnold, H. W. Sarkas, K. H. Bowen, C. Ludewigt, H. Haberland, and D. R. Worsnop, J. Chem. Phys. **92**, 3980(1990).
24. C. Silva, P. K. Walhout, K. Yokoyama, and P. F. Barbara, Phy. Rev. Lett. **80**, 1086(1998).
25. M. Assel, R. Laenen, and A. Laubereau, J. Chem. Phys. **111**, 6869(1999).
26. R. Laenen, T. Roth, and A. Laubereau, Phys. Rev. Lett. **85**, 50(2000).
27. P. Kambhampati, D. H. Son, T. K. Kee, and P. F. Barbara, J. Phys. Chem. A **106**, 2374(2002).
28. M. S. Pshenichnikov, A. Baltuska, and D. A. Wiersma, Chem. Phys. Lett. **389**, 171(2004).

29. Q.-B. Lu, J. S. Baskin, and A. H. Zewail, J. Phys. Chem. B **108**, 10509(2004).
30. L. Turi and D. Borgis, J. Chem. Phys. **117**, 6186(2002).
31. A. E. Bragg, J. R. R. Verlet, A. Kammrath, O. Cheshnovsky, and D. M. Neumark, Hydrated electron dynamics: From clusters to bulk. Science **306**, 669 (2004).
32. D. H. Paik, I. R. Lee, D. S. Yang, J. S. Baskin and A. H. Zewail, "Electrons in finite-sized water cavities: Hydration dynamics observed in real time", Science **306**, 672(2004).
33. L. Turi, W. S. Sheu, and P. J. Rossky, "Characterization of excess electrons in water-cluster anions by quantum simulations", Science **309**, 914 (2005).
34. H. Sambe, D. E. Ramaker, M. Deschênes, A. D. Bass, and L. Sanche, Phys. Rev. Lett. **64**, 523(1990).
35. Q.-B. Lu, A. D. Bass, and L. Sanche, Phys. Rev. Lett. **88**, 147601(2002).
36. B. C. Garrett, et al. Chem. Rev. **105**, 355 (2005).
37. Q.-B.Lu, and T. E. Madey, Phys. Rev. Lett. **82**, 4122(1999). J. Chem. Phys. **111**, 2861(1999).
38. Q.-B. Lu, and L. Sanche, Phys. Rev. Lett. **87**, 078501(2001); Phys. Rev. B **63**, 153403(2001); J. Chem. Phys. **115**, 5711(2001); ibid **120**, 2434(2004).
39. C.-R. Wang and Q.-B. Lu, "Real-Time Observation of Molecular Reaction Mechanism of Aqueous Halopyrimidines under UV/Ionizing Radiation", submitted.

Chapter 5

Real-time observation of reaction transition states of prehydrated electrons with nucleotides

Table of Contents Graphic

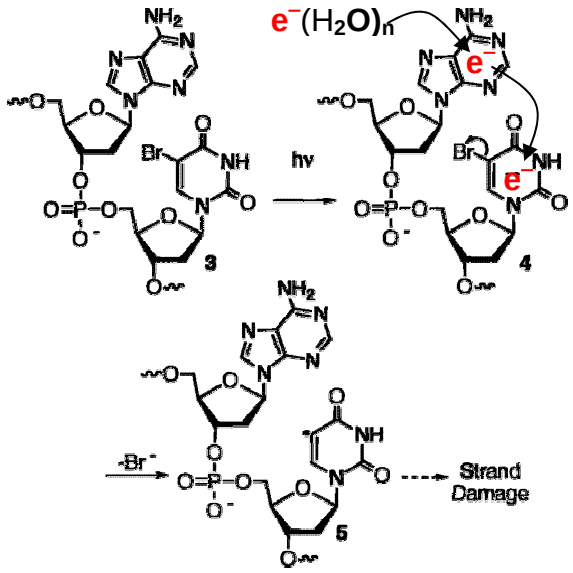

5.1 Introduction

As briefly mentioned in Chapter 1, one important feature of BrdU/IdU as radiosensitizing drugs is the dependence of its radio-/photosensitivity on DNA sequence [1-4]. The enhancement of the radio-/photosensitivity with respect to single- and double-strand breaks, creation of alkali-labile sites in duplex DNA containing BrdU/IdU was reported to be highly dependent on the identity of the nucleic bonded to the 5'- phosphate of BrdU/IdU [1-4]. It was observed that UV-irradiated duplexes containing the sequence 5'-dABrdU (-dAIdU) exhibited most significant DNA damage than analogous molecules containing either a 2'-deoxyguanosine (dG) or 2'-deoxycytidine (dC) in place of the adjacent 2'-deoxyadenosine (dA). Any true mechanism for the radio-/photosensitization of BrdU/IdU must be able to explain this important property. Some researchers suggested that it is due to the electron transfer from the neutral adenine base to BrdU/IdU [1-4]. The processes can be expressed as

$$dA + BrdU/IdU + h\nu\ (UV) \rightarrow dA^{+} + BrdU^{*-}/IdU^{*-} \qquad (5.1a)$$

$$BrdU^{*-}/IdU^{*-} \rightarrow Br^{-} + dU^{\bullet} \text{ or } I^{-} + dU^{\bullet} \qquad (5.1b)$$

However, in the UV light used with wavelengths above 300 nm, no absorption by the DNA bases occurs. In fact, *no dA^{+} cation, but neutral dA*, was detected in the experiments [2]. Moreover, this model does not agree with the expectation from the thermodynamic point of view, which would predict the most favorable electron transfer from the guanine base [5, 6]. So far, no proposed mechanism has been able to explain this interesting phenomenon well.

Based on our experimental results described in chapter 3 and 4, once BrdU capture electrons, the thus formed transition state, $BrdU^{*-}$, will quickly dissociate into a bromide anion and the highly reactive uracil radical. The latter will then cause single- and double-strand breaks, creation of alkali-labile sites, and RNA/DNA-protein photo-cross-linking [1-4, 7-13]. We proposed a new mechanism for the sequence selectivity of duplex DNA containing BrdU/IdU. In the first step, the DNA nucleoside-dA captures the precursor electron, e_{pre}^{-}, generated in ionizing radiation or by two-photon excitation of water in UV radiolysis; then the electron transfer from the DNA base anion-dA^{-} to BrdU/IdU, which is a very strong electron scavenger, to form the transition state $BrdU^{*-}/IdU^{*-}$. The transition state, $BrdU^{*-}/IdU^{*-}$ then quickly decay, forming the reactive uridine-yl radical to damage DNA. The processes can be expressed as:

$$H_2O + 2h\nu\ (UV) \rightarrow H_2O^{*} \rightarrow H_2O^{+} + e_{pre}^{-} \qquad (5.2a)$$

$$dA + e_{pre}^{-} \rightarrow \quad dA^{-} \tag{5.2b}$$

$$dA^{-} + BrdU/IdU \rightarrow dA + BrdU^{*-}/IdU^{*-} \tag{5.2c}$$

$$BrdU^{*-}/IdU^{*-} \rightarrow Br^{-} + dU^{\bullet} \text{ or } I^{-} + dU^{\bullet} \tag{5.2d}$$

Looking into the literature carefully, we have found that Nese et al. [14] have proposed a very similar mechanism, in which electron transfer from thymine and adenine electron adducts and their heteroatomprotonated forms formed by capture of hydrated electrons to 5-BrU was proposed. Inferred from their measurements of the dU radical yield in radiolysis of DNA base-BrU complexes, no electron transfer from the protonated guanine electron adduct to 5-BrU was observed. Instead, there is also electron transfer from the electron adduct of thymidine to cytosine and guanine which serve as electron sink [14]. To examine our proposed mechanism expressed in Eqs. (5.2a-5.2d), it is necessary to have real-time observation of the initial DNA base anions and the subsequent electron transfer to BrdU/IdU. This will require the time-resolved femtosecond laser spectroscopy because of the ultrashort lifetimes of e_{pre}^{-}.

An associated problem is related to the recent breakthrough in radiobiology that DNA strand breaks can be induced by low-energy (3-20 eV) electrons (LEEs) [15]. This is of great interest because low energy electrons are produced in significant numbers in ionizing radiation [16]. Most recently, both experimental and theoretical studies have shown that *free* electrons, even at energies approaching zero eV, can cause induced strand breaks in DNA by means of dissociative attachment (DA) of electrons [17-23]. A mechanistic understanding of LEE-induced DNA damage is of crucial importance for advancement of global models of cellular radiolysis and for the improvement of the efficacy of radiotherapy. There is a current interest in discussing the energy threshold for induction of DNA strand breaks by low energy electrons, and several different mechanisms for DNA strand breaks induced by LEEs have been proposed [20-23]. One central issue is regarding whether DNA strand breaks are initiated by electron attachment to DNA bases or to the phosphate group [22, 23]. If the DNA damage is initiated by electron attachment to DNA bases, then which base (s) is (are) the low-energy electrons attached to and what is the fate of the resultant anions? And what is the energy threshold for DNA strand breaks? So far, these experiments have only been done in dry plasmid DNA or in gas-phase DNA bases. Will the dissociative attachment of *weakly-bound* prehydrated electrons cause DNA damage in water? It has long been known that in aqueous environment, nucleotides can react with electrons generated in ionizing radiation to form their electron adducts, i.e., their anions [14, 24-26]. Very little is known, however, about the electron responsible for the formation of these anions and

the stability and subsequent fate of these primary anions in aqueous solution, except that they readily react with protons. The protonation of DNA base anions is a relatively slow process, however, occurring on the time scale of microsecond [27]. It is likely that our time-resolved femtosecond laser spectroscopic studies will give answers to these important questions.

5.2 Experimental Details

We used a Ti: sapphire laser system producing 120fs, 1mJ laser pulses centered at λ = 800 nm at a repetition rate of 1 kHz, two optical parametric amplifiers producing pump and probe pulses with wavelengths from visible to IR. The polarization of pump and probe pulses was set at the magic angle (54.7^{o}) to avoid contribution from polarization anisotropy duo to orientation motions of molecules. To avoid the direct absorption of the pump pulse by DNA bases, a pump wavelength 315 nm was used in these experiments. Excess electrons are produced by a two-photon excitation process in water [28-32]. The probe wavelengths 333 nm were selected to search the transition states ($dXMP^{*-}$) of the reactions of the mononucleotides of adenine, cytosine, guanine and thymidine, (dXMP, X= A, C, G and T) with the precursors to the hydrated electron [32]. Small pump pulse energy ($\leqslant$ 100nJ) was used to make the solvated electron signal negligible when detected at (probe) wavelength 333 nm and to avoid any nonlinear effects. Since the pump and probe wavelengths are now close to each other, a coherent 'spike' unavoidable appears at the delay time zero, which is clearly seen in the spectrum for the pure water. This "unwanted" spike, however, offers not only a visible and reliable in-situ reference for the pump-probe delay time zero but the instrument response function. In our experiments, an instrument response function of 300 fs was directly given by the full width at half maximum (FWHM) of the coherent spike. Transient absorption spectra of $dXMP^{*-}$ are corrected by subtracting the spectrum of the pure water (solvent) from the collected spectra; this also significantly reduces or completely removes the coherent spike from the spectra. All measurements are conducted at room temperature. The sample was held in a 5mm cell with a stirring bar to avoid any photoproduct accumulation. Ultrapure water with a resistivity of > 18 MΩ/cm was obtained from an ultrapure water system (Barnstead's Nanopure Diamond TOC Life Science). Nucleotides (dAMP, TMP, dGMP and dCMP) from Sigma-Aldrich were used as supplied.

5.3 Results and Discussion

Femtosecond transient absorption spectra of dXMPs obtained with λ_{pump} = 315 nm and λ_{probe} = 333 nm are shown in Figure 5.1(a) and (b). The interesting results observed are the following:

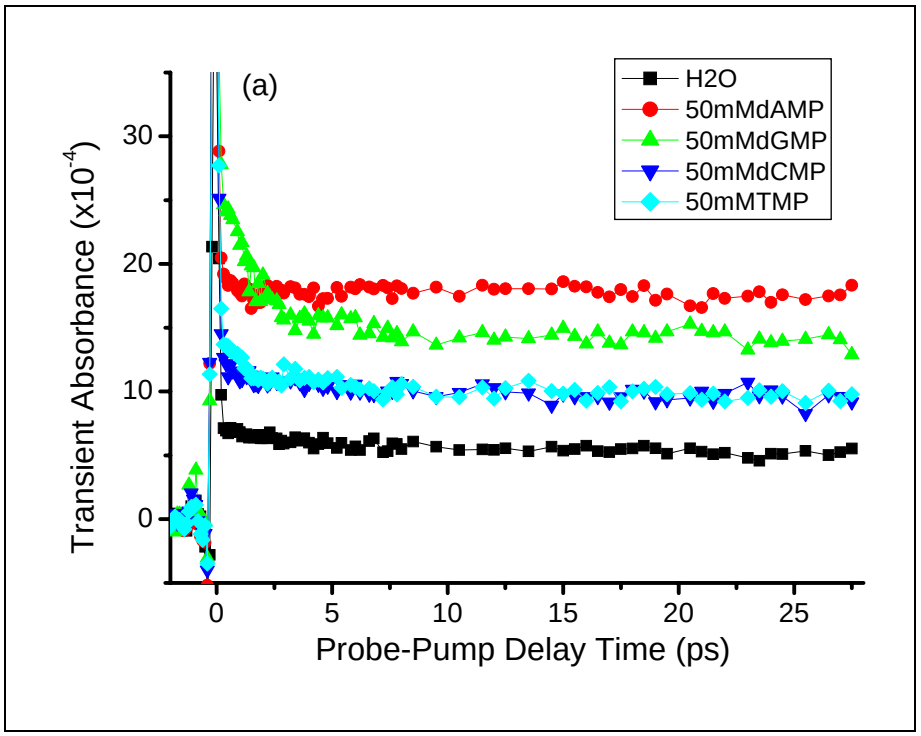

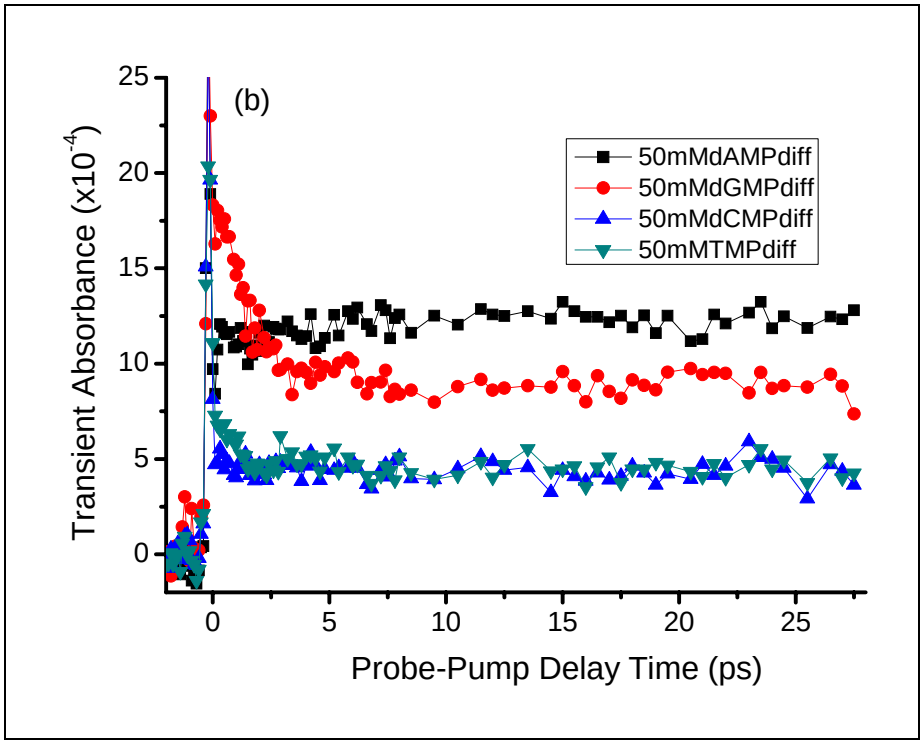

Figure 5.1. Femtosecond transient absorption spectra of 50mM dAMP, 50mM dGMP, 50mM dCMP and 50mM dTMP in water, pumped at 315nm and probed at 333nm: (a) original data, where the sharp peak at time zero is the coherence "spike" observed when λ_{pump} and λ_{probe} are close to each other; (b) spectra obtained after the subtraction of the spectrum for the pure water.

(1) The attachment of the ultrashort-lived prehydrated electrons to DNA bases was indeed observed, which takes place within the first picosecond after electronic excitation of water.
(2) dGMP has the largest probability of electron capture, among the 4 nucleotides.
(3) dAMP is the most effective for long-lived trapping of the precursor electron.
(4) Compared with dGMP and dAMP, the electron capture probabilities of dTMP and of dCMP are much smaller.
(5) $dGMP^{*-}$ and $dTMP^{*-}$ show quick decays in the first three picoseconds, indicating they are dissociative, i.e. dissociative attachments (DAs) of the prehydrated electron to dGMP and dTMP occur.

As shown in Figures 5.2 and 5.3 for dAMP and dGMP respectively, the transient absorption spectra of nucleotide anions simply exhibit a linear dependence on nucleotide concentration in the measured range of 25 to 100 mM. This indicates that the transient species must result from a single nucleotide molecule.

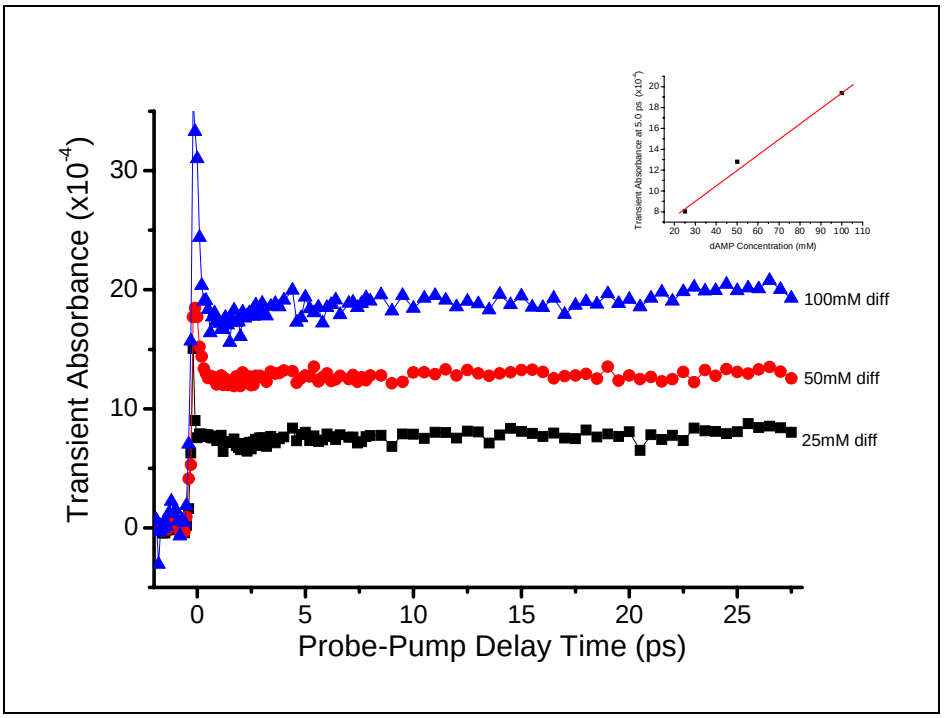

Figure 5.2. Femtosecond transition absorption spectrum of different concentration of dAMP in water, pumped at 315nm and probed at 333nm. The inset is the transient absorption at 5.0 ps as a function of dAMP concentration.

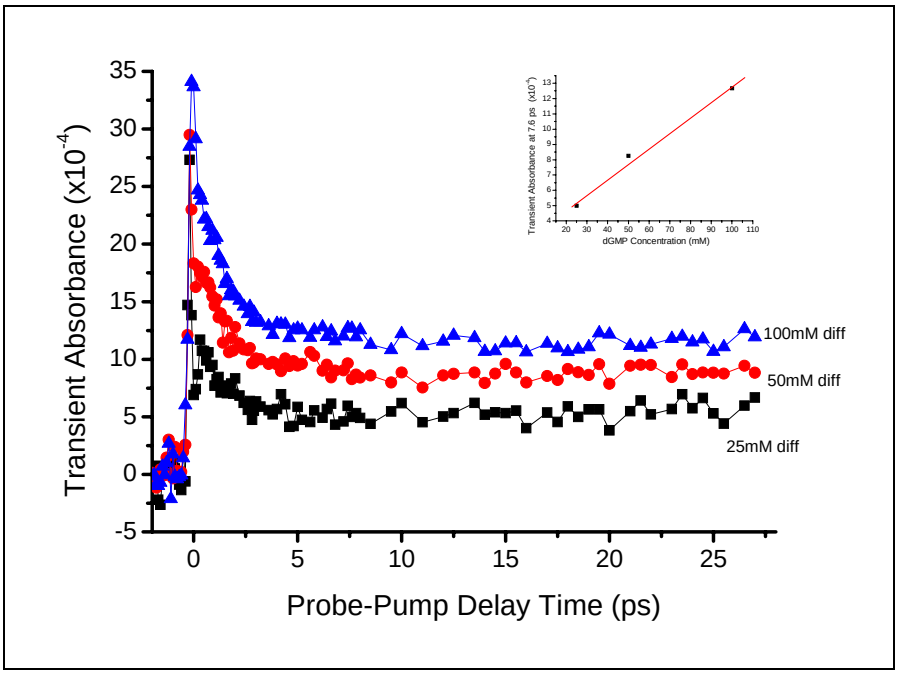

Figure 5.3. Femtosecond transition absorption spectrum of different concentration of dGMP in water, pumped at 315nm and probed at 333nm. The inset is the transient absorption at 7.6 ps as a function of dGMP concentration.

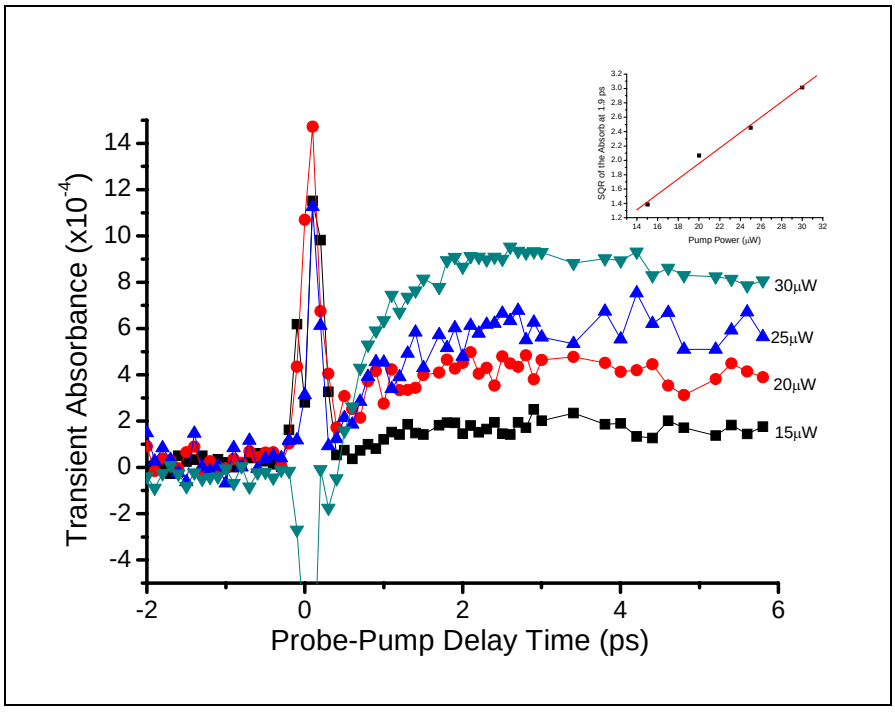

Figure 5.4. Femtosecond transient absorption spectra of 50mM dAMP in water, pumped at 315nm with various pulse energies and probed at 333 nm, after the subtraction of the spectrum for the pure water. The inset is the square root (SQRT) of the transient absorbance at 1.9 ps vs pump pulse energy.

As shown in Figure 5.4., moreover, the yield of the transient absorption of dAMP at 333nm shows a quadratic dependence on the pump pulse energy. This result confirms that the transition states result from the electrons, generated by two photon excitation of the water.

Most interestingly, the results in ***Figure 5.1*** *demonstrate that the transition state dGMP*$^{*-}$ *quickly decays in the first few picoseconds, indicating that DA occurs for dGMP. In contrast, dAMP*$^{*-}$ *is nondissociative, having a long lifetime.* These results indicate that the electron can be trapped by adenine for a long lifetime and can be efficiently transferred to BrdU/IdU when adenine is adjacent to BrdU/IdU. This can explain why the sequence 5'-dABrdU (-dAIdU) exhibits most significant enhancement in the induced radio-/photosensitivity (DNA damage) [1-4], though further confirmation of the electron transfer from dA^- to BrdU/IdU is yet to be done. This will also imply that adenine is an effective promoter for electron transfer reactions in biological systems. In contrast, guanine base exhibits the most effective dissociative electron attachment, which leads to the formation of a stable anion and a neutral counterpart. Thus, guanine was also observed to be the most effective electron sink [14]. The present results are drastically different from those reported for DNA bases in the gas phase, where dissociative attachment of free electrons (0-10 eV) to all four bases have been reported, including adenine, guanine, cytosine and thymine [17-23]. Our results indicate that DNA strand breaks can efficiently be induced by dissociative attachment of the weakly-bound precursor electron to the guanine base. Indeed, we have observed significant DNA single-strand breaks induced by the production of precursor electrons via two-photon excitation of water containing plasmid DNA [33]. Further experiments to measure the dissociation products of guanine by attachment of the precursor electron will be conducted with HPLC.

5.4 Conclusions

We have observed the ultrafast electron transfer reactions of the nucleotides (dAMP, dGMP, dCMP, and dTMP) with the precursors to the hydrated electrons. The present results indicate that adenine is the most efficient electron trapper and an effective electron transfer promoter. The observed results primarily explain the sequence selectivity of duplex DNA containing BrdU/IdU. Our results also imply that dissociative attachment of the precursor electron to guanine takes place rapidly, which can be an important mechanism for electron-induced DNA damage in radiation biology and radiotherapy of cancer. More work to confirm the electron transfer reactions between dA^- and BrdU/IdU and to measure the dissociation products of dAMP^{*-} will be of great interest.

References:

1. V. Murray and R. F. Martin, “The degree of ultraviolet light damage to DNA containing iododeoxyuridine or bromodeoxyuridine is dependent on the DNA sequence”, Nucleic Acids Research **17**, 2675(1989).
2. H. Sugiyama, Y. Tsutsumi, and I. Saito, “Highly sequence selective photoreaction of 5-Bromouracil-Containing Deoxyhexanucleotides” J. Am. Chem. Soc. **112**, 6720(1990).
3. G. P. Cook and M. M. Greenberg, “A novel mechanism for the formation of direct strand breaks upon Anaerobic photolysis of duplex DNA containing 5-Bromodeoxyuridine”, J. Am. Chem. Soc. **118**, 10025(1996).
4. T. Chen, G. P. Cook, and A. T. Koppisch, and M. M. Greenberg, “Investigation of the origin of the sequence selectivity for the 5-Halo-2’-deoxyuridine sensitization of DNA to Damage by UV-Irradiation”, J. Am. Chem. Soc. **122**, 3861(2000).
5. C. A. M. Seidel, A. Schulz, and M. H. M. Sauer, “Nucleobase-Specific Quenching of Fluorescent Dyes. 1. Nucleobase One-Electron Redox Potentials and Their Correlation with Static and Dynamic Quenching Efficiencies”, J. Phys. Chem. **100**, 5541(1996).
6. A. O. Colson and M. D. Sevilla, “Elucidation of primary radiation damage in DNA through application of ab initio molecular orbital theory”, Int. J. Radiat. Biol. **67**, 627(1995).
7. T. M. Dietz, R. J. V. Trebra, B. J. Swanson, and T. H. Koch, “Photochemical coupling of 5-bromouracil (BU) to a peptide linkage. A model for BU-DNA protein photocrosslinking”, J. Am. Chem. Soc. **109**, 1793(1987).
8. K. L. Wick and K. S. Matthews, “Interactions between lac repressor protein and site-specific bromodeoxyuridine-substituted operator DNA. Ultraviolet footprinting and protein-DNA cross-link formation”, J. Biol. Chem., **266**, 6106(1991).
9. E. E. Blatter, Y. W. Ebright, and R. H. Ebright, “Identification of an amino acid–base contact in the GCN4–DNA complex by bromouracil-mediated photocrosslinking”, Nature **359**, 650(1992).
10. M. C. Willis, B. J. Hicke, O. C. Uhlenbeck, T. R. Cech and T. H. Koch, “Photocrosslinking of 5-iodouracil-substituted RNA and DNA to proteins”, Science **262**, 1255(1993).
11. B. J. Hicke, M. C. Willis, T. H. Koch, and T. R. Cech, “Telomeric Protein-DNA Point Contracts Identified by Photo-Crosslinking Using 5-Bromodeoxyuridine”, Biochemistry, **33**, 3364(1994).
12. M. M. Paz, G. S. Kumar, M. Glover, M. J. Waring, and M. Tomasz, “Mitomycin dimers: polyfunctional cross-linkers of DNA”, J. Med. Chem. **47**, 3308(2004)
13. N. Reguart, N. Vinolas, F. Casas, J. M. Gimferrer, C. Agusti, M. Molina, R. Martin-Richard, A. Sanchez-Reyes, and P. Gascon, “Integrating concurrent navelbine and cisplatin to hyperfractionated radiotherapy in locally advanced non-small cell

lung cancer patients treated with induction and consolidation chemotherapy: feasibility and activity results", Lung Cancer **45**, 67(2004).
14. C. Nese, Z. Yuan, M. N. Schuchmann, and C. V. Sonntag, "Electron transfer from nucleobase electron adducts to 5-bromouracil. Is guanine an ultimate sink for the electron in irradiated DNA?" Int. J. radiat. Biol. **62**, 527(1992).
15. B. Boudaiffa, P. Cloutier, D. Hunting, M. A. Huels and L. Sanche, "Resonant Formation of DNA strand breaks by low-energy (3-20 eV) electrons", Science **287**, 1658(2000).
16. J. A. Laverne and S. M. Pimblott, "Electron-energy-loss distributions in solid, dry DNA", Radiat. Res. **141**, 208 (1995).
17. S. Gohlke, H. Abdoul-Carime, E. Illenberger, "Dehydrogenation of adenine induced by slow (< 3 eV) electrons", Chem. Phys. Lett. **380**, 595-599(2003); H. Abdoul-Carime, S. Gohlke, E. Fischbach, J. Scheike, E. Illenberger, "Thymine excision from DNA by subexcitation electrons", Chem. Phys. Lett. **387**, 267 (2004).
18. F. Martin, P. D. Burrow, Z. L. Cai, P. Cloutier, D. Hunting, L. Sanche, "DNA strand breaks induced by 0-4 eV electrons: The role of shape resonances", Phys. Rev. Lett. **93**, 068101(2004).
19. H. Abdoul-Carime, J. Langer, M. A. Huels, E. Illenberger, "Decomposition of purine nucleobases by very low energy electrons", Eur. Phys. J. D**35**, 399(2005).
20. C. Konig. J. Kopyra, I. Bald, E. Illenberger, "Dissociative electron attachment to phosphoric acid esters: The direct mechanism for single strand breaks in DNA", Phys. Rev. Lett. **97**, 018105(2006).
21. P. D. Burrow, G. A. Gallup, A. M. Scheer, S. Denifl, S. Ptasinska, T. Mark, P. Scheier, "Vibrational Feshbach resonances in uracil and thymine", J. Chem. Phys. **124**, 124310(2006).
22. Y. Zheng, I. R. Wagner and L. Sanche, "DNA damage induced by low-energy electrons: electron transfer and diffraction", Phys. Rev. Lett. **96**, 208101(2006).
23. J. Gu, Y. Xie, and H. F. Schaefer, "Near 0 eV Electron Attach to Nucleotides", J. Am. Chem. Soc. **128**, 1250(2005); X. Bao, J. Wang, J. Gu, and J. Leszczynski, "DNA strand breaks induced by near-zero-electronvolt electron attachment to pyrimidine nucleotides", Proc. Natl. Acad. Sci. USA **103**, 5658(2006).
24. E. Hayon, "Optical-Absorption Spectra of Ketyl Radicals and Radical Anions of some Pyrimidines", J. Chem. Phys. **51**, 4881(1969).
25. A. Hissung, and C. V. Sonntag, "The reaction of the 2'-deoxyadenosine electron adduct in aqueous solution. The effects of the radiosensitizer þ−nitroacetophenone. A pulse spectroscopic and pulse conductometric study", Int. J. Radiat. Biol **39**, 63(1981).
26. L. P. Candeias and S. Steenken, "Electron Adducts of Adenine Nucleosides and Nucleotides in Aqueous Solution: Protonation at Two Carbon Sites (C2 and C8) and Intra- and Intermolecular Catalysis by Phosphate", J. Phys. Chem. **96**, 937(1992).

27. C. V. Sonntag, “The Chemical Basis of Radiation Biology”, (London-New York-Philadelphia 1987).
28. A. Migus, Y. Gauduel, J. L. Martin, and A. Antonetti, Phys. Rev. Lett. **58**, 1559(1987).
29. F. H. Long, H. Lu, and K. B. Eisenthal, Phys. Rev. Lett. **64**, 1469(1990).
30. R. Laenen, T. Roth and A. Laubereau, Phys. Rev. Lett. **85**, 50(2000).
31. Q.-B. Lu, J. S. Baskin, and A. H. Zewail, J. Phys. Chem. B **108**, 10509(2004)**.**
32. C.-R. Wang, A. Hu, and Q.-B. Lu, J. Chem. Phys. **125**, 241102(2006).
33. Q.-B. Lu, “Molecular Reaction Mechanisms of Combination Treatments of Low-Dose Cisplatin with Radiotherapy and Photodynamic Therapy”. J. Med. Chem. 2007, in press.

Chapter 6

Conclusions

We have performed state-of-the-art time-resolved femtosecond laser spectroscopic experiments on a chemically, biologically and practically significant system, namely halopyrimidines, and have obtained the first, real-time observation of the ultrafast electron transfer (ET) reactions involving the short-lived precursor to the hydrated electron, e_{pre}^-, that leads to the formation of the transient CldU*$^-$, BrdU*$^-$, IdU*$^-$ states. The latters dissociate into halogen anions and a highly reactive radical that then causes DNA damage and cell death.

This is the first, direct observation of the ultrafast ET reactions of the precursor to the solvated electron with biologically important molecules, and our results lead to a new mechanism of action at the molecular level of halopyrimidines as candidate drugs for radiotherapy of cancer. We find that the ET reaction efficiency is in the order of CldU<BrdU << IdU. This is due to the availability of two precursor states for DEA to IdU, of one precursor state for DEAs to BrdU and CldU, and no precursors for DEA to FdU. Among halopyrimidines, *IdU should be explored as the most promising radiosensitizing drug.* Efforts should be made to promote the ET reactions of these radiosensitisers with precursor electrons in order to enhance the therapeutic efficacy.

Moreover, our results have revealed the physical nature of the e_{pre}^- states and show direct evidence of the long-sought wet electron in water, where halopyrimidines were indeed employed as quantum-state-specific probe molecules. We also provide direct evidence of the excited-state model of the long-sought “wet” electron that has a lifetime of ~0.54 ps.

These findings will also have a broader significance as they indicate that nonequilibrium precursor electrons may play an important role in electron-initiated reactions in many biological and environmental systems. The precursor electron is a general product in ionizing/UV radiation. Our results have challenged a long accepted mechanism that long-lived hydrated electrons would be responsible for the radical formation in reactions with halogen-containing molecules. In summary, this study can have clear significance for understanding of the role of water in electron-initiated reactions and radical chemistry in many chemical, biological and environmental systems, ranging from breakups of environmentally important halogenated molecules to the activation of halogen-containing anticancer drugs.

The ultrafast electron transfer reactions of nucleotides with the prehydrated electron

primarily explain the sequence selectivity of duplex DNA containing BrdU/IdU. The results also imply that dissociative attachment of the precursor electron to guanine takes place rapidly, which can be an important mechanism for radiation-induced DNA damage in ionizing radiation and radiotherapy of cancer. Future work will be done (1) to demonstrate the electron transfer reactions between the electron adduct of nucleotides (especially dA^{-}) and BrdU/IdU, (2) to clarify the dissociation products of $dGMP^{*-}$, and (3) to precisely chracterize the DNA damage induced by the reactions of prehydrated electrons generated in ionizing radiation.

With our femtosecond laser spectroscopy, it is promising for us to (1)determine the precise reaction mechanism at the molecular level of BrdU and IdU as radio-/photosensitizing drugs for cancer therapy and DNA/RNA-protein photocrosslinking, (2) to identify the molecular triggers for enhancement or control of the reactivity of BrdU and IdU, and (3) to make these candidate anticancer drugs more effective so that the BrdU and IdU could go through the final clinical trials, taking advantage of our mechanistic understanding of the reactions of these molecules at the *molecular* level.